New insights in the assessment of right ventricular function: an echocardiographic study

Avin Calcutteea

Department of Public Health and Clinical Medicine
Umeå University, 2013

New insights in the assessment of right ventricular function: an echocardiographic study

Avin Calcutteea

2013

Department of Public Health and Clinical Medicine
Umeå University
Umeå, 2013

Responsible publisher under swedish law: the Dean of the Medical Faculty

New Series No: 1551
ISBN: 978-91-7459-561-1
ISSN: 0346-6612
E-version available at http://umu.diva-portal.org/
Printed by: Print & Media, Umea University
Umeå, Sweden 2013

"Education is a progressive discovery

of our own ignorance"

To my parents

Table of contents

ABSTRACT

Background: The right ventricle (RV) is multi-compartmental in orientation with a complex structural geometry. However, assessment of this part of the heart has remained an elusive clinical challenge. As a matter of fact, its importance has been underestimated in the past, especially its role as a determinant of cardiac symptoms, exercise capacity in chronic heart failure and survival in patients with valvular disease of the left heart. Evidence also exists that pulmonary hypertension (PH) affects primarily the right ventricular function. On the other hand, previous literature suggested that severe aortic stenosis (AS) affects left ventricular (LV) structure and function which partially recover after aortic valve replacement (AVR). However, the impact of that on RV global and segmental function remains undetermined.

Objectives: We sought to gain more insight into the RV physiology using 3D technology, Speckle tracking as well as already applicable echocardiographic measures. Our first aim was to assess the normal differential function of the RV inflow tract (IT), apical and outflow tract (OT) compartments, also their interrelations and the response to pulmonary hypertension. We also investigated the extent of RV dysfunction in severe AS and its response to AVR. Lastly, we studied the extent of global and regional right ventricular dysfunction in patients with pulmonary hypertension of different aetiologies and normal LV function.

Methods: The studies were performed on three different groups; (1) left sided heart failure with (Group 1) and without (Group 2) secondary pulmonary hypertension, (2) severe aortic stenosis and six months post AVR and (3) pulmonary hypertension of different aetiologies and normal left ventricular function. We used 3D, speckle tracking echocardiography and conventionally available Doppler echocardiographic transthoracic techniques including M-mode, 2D and myocardial tissue Doppler. All patients' measurements were compared with healthy subjects (controls). Statistics were performed using a commercially available SPSS software.

Results: 1- Our RV 3D tripartite model was validated with 2D measures and eventually showed strong correlations between RV inflow diameter (2D) and end diastolic volume (3D) ($r=0.69$, $p<0.001$) and between tricuspid annular systolic excursion (TAPSE) and RV ejection fraction (3D) ($r=0.71$, $p<0.001$). In patients (group 1 & 2) we found that the apical ejection fraction (EF) was less than the inflow and outflow (controls: $p<0.01$ & $p<0.01$, Group 1: $p<0.05$ & $p<0.01$ and Group 2: $p<0.05$ & $p<0.01$, respectively). Ejection fraction (EF) was reduced in both patient groups ($p<0.05$ for all compartments). Whilst in controls, the inflow compartment reached the minimum volume 20 ms before the outflow and apex, in Group 2 it was virtually

simultaneous. Both patient groups showed prolonged isovolumic contraction (IVC) and relaxation (IVR) times ($p<0.05$ for all). Also, in controls, the outflow tract was the only compartment where the rate of volume fall correlated with the time to peak RV ejection ($r = 0.62$, $p = 0.03$). In Group 1, this relationship was lost and became with the inflow compartment ($r = 0.61$, $p = 0.01$). In Group 2, the highest correlation was with the apex ($r=0.60$, $p<0.05$), but not with the outflow tract.

2- In patients with severe aortic stenosis, time to peak RV ejection correlated with the basal cavity segment ($r = 0.72$, $p<0.001$) but not with the RVOT. The same pattern of disturbance remained after 6 months of AVR ($r = 0.71$, $p<0.001$). In contrast to the pre-operative and post-operative patients, time to RV peak ejection correlated with the time to peak outflow tract strain rate ($r = 0.7$, $p<0.001$), but not with basal cavity function. Finally in patients, RVOT strain rate (SR) did not change after AVR but basal cavity SR fell ($p=0.04$).

3- In patients with pulmonary hypertension of different aetiologies and normal LV function, RV inflow and outflow tracts were dilated ($p<0.001$ for both). Furthermore, TAPSE ($p<0.001$), inflow velocities ($p<0.001$), basal and mid-cavity strain rate (SR) and longitudinal displacement ($p<0.001$ for all) were all reduced. The time to peak systolic SR at basal, mid-cavity ($p<0.001$ for both) and RVOT ($p=0.007$) was short as was that to peak displacement ($p<0.001$ for all). The time to peak pulmonary ejection correlated with time to peak SR at RVOT ($r=0.7$, $p<0.001$) in controls, but with that of the mid cavity in patients ($r=0.71$, $p<0.001$). Finally, pulmonary ejection acceleration (PAc) was faster ($p=0.001$) and RV filling time shorter in patients ($p=0.03$) with respect to controls.

Conclusion: RV has distinct features for the inflow, apical and outflow tract compartments, with different extent of contribution to the overall systolic function. In PH, RV becomes one dyssynchronous compartment which itself may have perpetual effect on overall cardiac dysfunction. In addition, critical aortic stenosis results in RV configuration changes with the inflow tract, rather than outflow tract, determining peak ejection. This pattern of disturbance remains six month after valve replacement, which confirms that once RV physiology is disturbed it does not fully recover. The findings of this study suggest an organised RV remodelling which might explain the known limited exercise capacity in such patients. Furthermore, in patients with PH of different aetiologies and normal LV function, there is a similar pattern of RV disturbance. Therefore, we can conclude that early identification of such changes might help in identifying patients who need more aggressive therapy early on in the disease process.

LIST OF PAPERS

I. Calcutteea A, Chung R, Linqvist P, Hodson M, Henein MY. Differential Right ventricular regional function and the effect of pulmonary hypertension: three dimensional echo study. Heart 2011;97:1004-11.

II. Calcutteea A, Holmgren A, Lindqvist P, Henein MY. Organised right ventricular remodelling in aortic stenosis even after valve replacement. Int J Cardiol 2012. Manuscript accepted for publication in a concise letter format.

III. Calcutteea A, Lindqvist P, Soderberg S, Henein MY. Global and regional right ventricular disturbances in pulmonary hypertension. Submitted

ABBREVIATIONS & ACRONYMS

RV	Right ventricle
LV	Left ventricle
OT	Outflow tract
RVOT	Right ventricular outflow tract
LVOT	Left ventricular outflow tract
IT	Inflow tract
PV	Pulmonary valve
TV	Tricuspid valve
RA	Right atrium
LA	Left atrium
IVC	Inferior vena cava
SVC	Superior vena cava
ECG	Electrocardiogram
IVCT	Isovolumic contraction time
IVRT	Isovolumic relaxation time
PH	Pulmonary hypertension
PAH	Pulmonary arterial hypertension
RAP	Right atrial pressure
LAP	Left atrial pressure
IPAH	Idiopathic pulmonary arterial hypertension
FPAH	Familial pulmonary arterial hypertension
APAH	Associated pulmonary arterial hypertension
CTEPH	Chronic thromboembolic pulmonary hypertension

TR	Tricuspid regurgitation
TAPSE	Tricuspid annular plane systolic excursion
RCA	Right coronary artery
PVR	Pulmonary vascular resistance
COPD	Chronic obstructive pulmonary disease
MRI	Magnetic resonance imaging
SPECT	Single-photon emission computed tomography
PASP	Pulmonary artery systolic pressure
MPAP	Mean pulmonary artery pressure
2DE	Two-dimensional echocardiography
CW	Continuous wave
V	Velocity
PW	Pulse wave
E	Early filling component
A	Late filling component
ET	Ejection time
FT	Filling time
MPI	Myocardial performance index
DTI	Doppler tissue imaging
S’	Systolic velocity of Doppler tissue imaging
e’	Early diastolic filling velocity from Doppler tissue imaging
a’	Atrial filling velocity from Doppler tissue imaging
3DE	Three dimensional echocardiography
CMR	Cardiac magnetic resonance
PA	Pulmonary pressure
PR	Pulmonary regurgitation

PAc	Pulmonary ejection acceleration
PAcT	Pulmonary artery acceleration time
WU	Woods units
Edpd	Early diastole peak pressure drop
Pv	Peak velocity
VTI	Velocity time integral
PCWP	Pulmonary capillary wedge pressure
SV	Stroke volume
CO	Cardiac output
RHC	Right heart catheterisation
AS	Aortic stenosis
AVR	Aortic valve replacement
A4Ch	Apical 4-chamber plane
EF	Ejection fraction
STE	Speckle tracking echocardiography
SR	Strain rate
ROI	Region of interest
GLSRs	Global systolic longitudinal left ventricular strain rate
EDD	End-diastolic diameter
ESD	End-systolic diameter
IVST	Interventricular septal wall thickness
PWT	Posterior wall thickness
ESV	End-systolic volume
EDV	End-diastolic volume
AccT	Acceleration time
DeccT	Deceleration time

TAD	Tricuspid annular diameter
D	Displacement
TSR	Time to peak strain rate
TPD	Time to peak displacement

Figures and graphs in the introduction were reproduced by permission from the following publishers and authors:

1. Henein MY, Zhao Y, Nicholl R, Sun L, Khir AW, Franklin K, et al. The human heart: application of the golden ratio and angle. Int J Cardiol 2011;150:239-42.

2. Greenbaum RA, Ho SY, Gibson DG, Becker AE, Anderson RH. Left ventricular fibre architecture in man. Br Heart J 1981;45:248-63.

3. Nagel E, Stuber M, Hess OM. Importance of the right ventricle in valvular heart disease. Eur Heart J 1996;17:829-836. Review.

INTRODUCTION

I. The importance of the right ventricle

The right ventricle (RV) having a very complex structural geometry is often overlooked and hence undermining its importance in contributing to the overall cardiac function. RV function has been shown to be a sensitive predictor of exercise tolerance and is also a major determinant of clinical symptoms in chronic heart failure as well as peri-operative and post-operative survival outcome [1, 2]. Identifying the most sensitive markers of RV dysfunction is of immense importance in daily clinical practice. RV function may be impaired either by primary right sided heart disease, or secondary to left sided cardiomyopathy or valvular heart disease. For instance, pressure or volume overload from an incompetent valve or muscle pathology can affect the RV function. Coronary artery disease may also lead to RV dysfunction when the right coronary artery is occluded. Moreover, in congenital malformation of the heart, the RV may also be affected, particularly when it becomes the main pumping chamber supporting the systemic circulation, e.g. congenitally corrected transposition of the great arteries or univentricular repair at surgery [3]. Lastly, right to left shunting may have perpetual effect on the RV in the form of dilation and impairment through volume overload as in the case with atrial and ventricular septal defects [3, 4]. Based on the above, it is clear that understanding the anatomy as well as normal and abnormal physiology of the right heart is of significant importance.

II. Right heart anatomy

The right ventricle is located immediately behind the sternum and anteriorly positioned to the left ventricle (LV). The inlet part of the RV is much smaller than the LV and its muscle mass is approximately 1/6 that of the LV, which can be explained by different loading conditions. In normal hearts, the right ventricle pumps against a pressure of 30 mmHg which is ¼ that of the LV, a fact that clearly shows that the RV and LV are designed differently [5]. Consequently, the LV wall which supports the systemic circulation is thicker (6-11mm) than that of the RV (3-4mm) which supports the low pressure pulmonary circulation [6]. When viewed from the front, the RV is more triangular in shape and it curves over the near conical shape of the LV making the cavity a crescent – like shape in cross section. When viewed from the apex, the right edge of

the RV is sharp, forming the acute margin of the heart. There is a 'cross over' relationship between the right ventricular outflow tract (RVOT) and left ventricular outflow tract (LVOT) due to the curvature of the ventricular septum which places the right ventricular outflow tract antero-cephalic to that of the LV outflow tract. The pulmonary valve, which guards the RVOT, is the most superiorly situated of the cardiac valves and this is due to the musculature of the subpulmonary infundibulum, free of trabeculations, which raises the valve above the ventricular septum [3]. The pulmonary valve (PV) marks the superior margin of the RV while the tricuspid valve (TV) marks its right margin and its apex is frequently inferior to that of the left ventricle. Morphologically the RV is composed of several anatomical segments that can be described in terms of three component parts namely the inlet, apical trabecular and outlet or right ventricular outflow tract as suggested by Goor and Lillehei [7]. Whilst the apex is virtually an immobile part of the ventricle and heavily trabeculated, the inflow and outflow tracts (IT and OT) are separated by a thick intracavitary muscle band called crista supraventricularis [8]. The moderator band is another intracavitary muscle band which is attached to the outflow tract and runs from the septum to the anterior RV free wall [9]. The right ventricular inflow and outflow axis angle is approximately 37.5°, [10] [figure 1] an anatomical fact that requires the outflow tract to contribute significantly to the overall RV systolic function. The fibre architecture of the left and right ventricle is different [11, 12]. The difference in the myocardial fibre architecture of the two pumps explains the difference in shape and dynamics of the two ventricles. The predominant muscle layer of the LV is composed mainly of circumferential or spiral fibres and longitudinally directed fibres are located in the subendocardial and subepicardial layers. On the other hand, at the inflow tract of the RV, circumferential or spiral fibres are mainly located in the subepicardium whereas in the subendocardium there are mainly longitudinal fibres [11], [Figure 2].

The RV outflow tract consists of longitudinal fibres at both the subendocardium and subepicardium which are overlaid by circumferential fibres running at right angle to the outlet long axis, which can be traced to the crista supraventricularis and to the anterior sulcus, serving to bind the two ventricles together. The outflow tract, which is anatomically and functionally different from the rest of the RV, can be described as a bulbar musculature [13, 14]. However the functional role of this part of the RV is not fully understood [15] but is believed to protect the pulmonary circulation during pressure rise in systole [14, 16] while the same volume of blood is ejected from the thin walled RV and the much thicker walled LV. Three dimensional studies of

RVOT has been performed in order to characterise its exact shape as well as providing more accurate assessment of cardiac output [17].

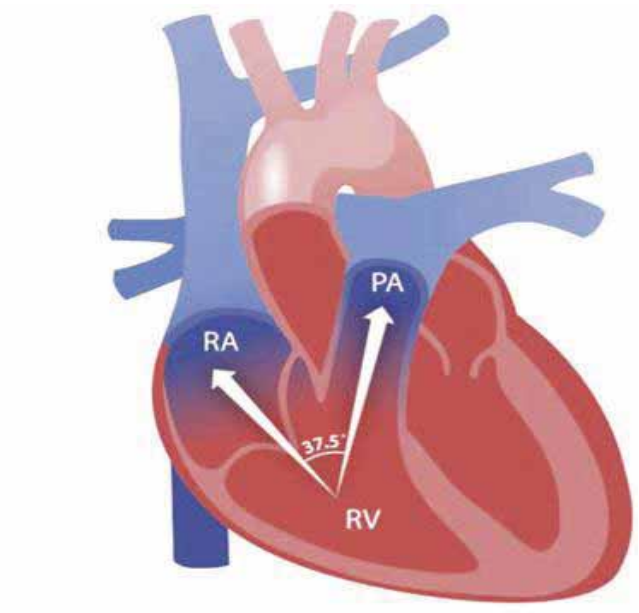

Figure 1. Diagram showing the angle between inflow and outflow tract axes of the right ventricle. RA: right atrium; PA: pulmonary artery, from Henein et al. editorial published in International Journal of Cardiology 2011;150:239-242.

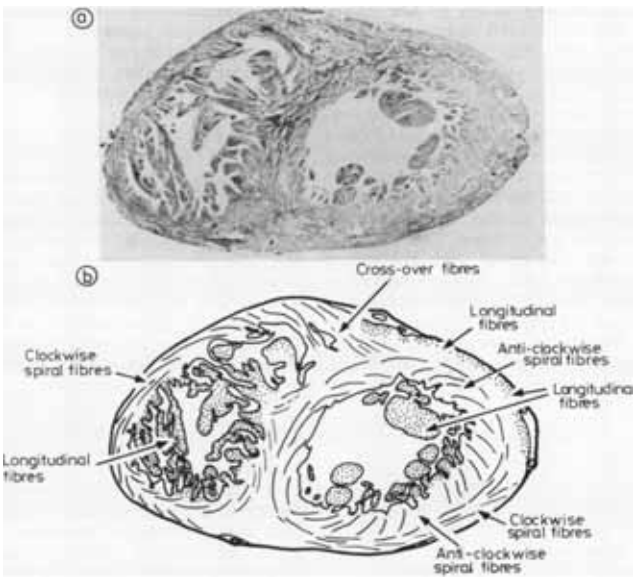

Figure 2. Myocardial fibre architecture of the two pumps (LV and RV), from Greenbaum et al. published in Br Heart J 1981;45:248-63

III. Right heart physiology and its response to increased afterload

Right ventricular systole

The RV wall motion is complex [18, 19]. During systole, there is a longitudinal shortening from base to apex, at the inflow tract and a radial motion towards the interventricular septum. Rotational or squeezing effect of the ventricle occurs from additional circumferential motion [20]. The subepicardial fibres of the inflow tract, allow the ventricle to move in a circumferential direction and occurs mainly during the isovolumic contraction phase, and the longitudinal shortening of the RV occurs mainly during the ejection phase and is controlled by the subendocardial fibres. The wide angle between the inflow and outflow has significant implication on the overall function of the RV with the inlet part starting shortening 20 milliseconds before the outlet part in order to keep its peristaltic movement, [21] which is crucial to keep the intracavitary circulation and to allow blood to be directed out into the

pulmonary arterial tree. Furthermore, it seems that the circumferential contraction of the outflow tract is important in order to maintain high tension during systole, which results in the infundibular subvalvular support to the pulmonary valve unidirectional function. Finally, the interventricular septum contributes to both the LV and RV function [22] and is a major determinant of maximal RV function [23], although its specific contribution to RV function is not fully understood in both normal and abnormal hearts. However, there is evidence which suggests that the septum compensates for any drop in RV free wall function, as is the case after open heart surgery [24].

Right ventricle and Right atrium physiological relationship

The right atrium (RA) receives the venous return, deoxygenated blood, from the inferior and superior vena cava (IVC and SVC) as well as the coronary sinus. It assists in filling the right ventricle (diastolic function) by three mechanisms [25].

(1) It acts as a reservoir for systemic venous return when the tricuspid valve is closed.
(2) It acts as a passive conduit when the tricuspid valve is open in early diastole.
(3) During late diastole when the atrium contracts, it acts as an active conduit.

Patients with acute injury to the right ventricle, notably in the form of myocardial infarction, results in RV diastolic dysfunction with dilatation of the RA due to elevated filling pressures, and clinically apparent jugular venous distension [26-28]. There are a number of acute and chronic conditions that are associated with RV diastolic dysfunction, such as pressure and volume overload pathologies, primary lung disease, ischaemic lung disease, congenital heart disease, cardiomyopathies, LV dysfunction, systemic diseases and finally the physiological ageing process [29].

Right heart vs. left heart

Right ventricular ejection fraction is dependent on right ventricular afterload and thus, on left ventricular or left atrial filling pressures [30-33]. An increase in left ventricular afterload is compensated for by an increase in mass to reduce left ventricular fibre stress with the overall function maintained. The right ventricle, on the other hand, is more sensitive to changes in pressure overload, probably due to its smaller muscle mass and thus higher wall stress of a given

load which affects its overall function. Figure 3, reproduced by E.Nagel et al. in a review article, [34] shows that right ventricular ejection fraction is reduced by approximately 10% (55 to 45%) when right ventricular afterload is doubled from 25 to 50 mmHg. Doubling of left ventricular afterload from 125 to 250 mmHg results in a similar reduction in its ejection fraction from 70 to 60%. The data in the graph below were taken from previous studies [30, 31, 35-39].

Although there are significant differences in structure and function of the two ventricles, the two pumps have similar electrical and mechanical roles. The right ventricle starts contracting shortly after the Q-wave of the ECG (electrocardiogram), which results in a period of electromechanical delay, significantly shorter than that of the LV [40]. A possible explanation of this change could be due to the fact that there is significant shape change of the LV, occurring during the isovolumic contraction time (IVCT), compared to the direct longitudinal shortening of the RV, during the same phase of the cardiac cycle [41]. Again the two ventricles differ in their behaviour in early diastole, where the RV has a very short isovolumic relaxation time (IVRT ≤ 60 ms) compared to that of the left ventricle which is approximately 80 milliseconds. These differences are also due to the early shape change before mitral valve opening, on the left side, as compared to tricuspid valve opening on the right side and the relatively low pressure differences between RA and RV during IVRT. Both LV and RV show the same filling components i.e. the early diastolic component and a late diastolic one (atrial contraction). The main difference in the filling pattern of the two ventricles is the velocity, which reflects the loading conditions of the two ventricles, being significantly higher in the left ventricle than in the right ventricle. Moreover, along with the difference in afterload of the two chambers, the ejection velocities also differ significantly with higher velocities in the LV. Despite such differences between the two ventricles, the small and sensitive RV is capable of filling and pumping blood at the same rate and volume as the thick walled LV. This can be explained by comparing the characteristics of the pulmonary and systemic circulation as described below [5].

- When compared to the systemic pressure and resistance, the pulmonary artery pressure and pulmonary vascular resistance are only approximately 1/6 that of the systemic values.
- Systemic arterial distensibility is lower than the pulmonary arterial distensibility.
- The pulmonary artery pulse amplitude is lower than the systemic pulse amplitude.
- There is lower peripheral pulse wave reflection in the pulmonary arteries than that in the systemic circulation.

- Pulmonary arteries do not exhibit increasing stiffness between central and peripheral sites.

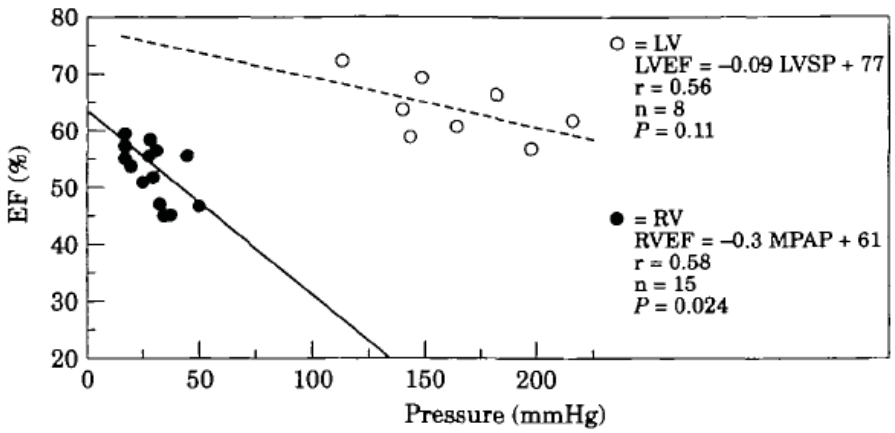

Figure 3. Relationship between angiographic RV (●) ejection fraction (EF_{RV}) and mean pulmonary artery pressure (MPAP), as well as left ventricular (○) ejection fraction and peak systolic pressure (LVSP). The slope of the regression line is steeper for the right ventricle than the left ventricle, indicating a higher load-sensitivity of the right ventricle. Data are taken from the literature; each data point represents one different study, from E.Nagel et al. review published in European Heart Journal 1996;17:829-836.

Effect of pressure overload on the right ventricle

The relationship between pulmonary artery pressure and RV function is complicated [8, 30] as it depends on factors such as age, gender, primary or secondary pulmonary hypertension (PH), acute or chronic elevation of pulmonary pressures, volume overload, raised right atrial pressure (RAP) and type of myocardial diseases [34, 42, 43]. Chronic elevation of pulmonary artery pressure is the commonest cause of pressure overload on the RV. Patients with severe left heart problems, such as mitral valve disease or left ventricular disease are described as having post-capillary rise in pulmonary pressure and those with idiopathic, familial or associated pulmonary arterial hypertension (IPAH, FPAH and APAH) secondary to pulmonary disease or chronic

thromboembolic pulmonary hypertension (CTEPH), are described as having pre-capillary pulmonary hypertension. While the pathologies of increased afterload are different, their effect on the RV could be similar. The thin walls of the RV make the cavity sensitive to alterations in pulmonary artery pressure. When afterload increases slowly, the RV chamber adapts and compensates by dilating and developing hypertrophy. In some cases, such as pulmonary embolism where the pulmonary pressures can significantly increase acutely, the RV enlarges and may cause elevated RV end diastolic and right atrial pressures leading to significant tricuspid regurgitation (TR) and right heart failure with its known poor outcome [44]. Some authors have distinguished between patients with RV pressure overload with and without tricuspid regurgitation [38, 39, 45] and found higher mean pulmonary artery pressures and lower right ventricular ejection fraction in those with tricuspid regurgitation [38], although there is a low impedance leak with regurgitation into the right atrium.

Effect of left heart valve diseases on the right ventricle

Mitral valve disease generally influences the right ventricle more than aortic valve disease [35, 46]. Left atrial volume overload in mitral insufficiency and pressure overload in mitral stenosis may cause an increase in pulmonary venous pressure with or without an increase in vascular resistance. This will have its consequences as an increased afterload to the right ventricle and thus impairment of its function and development of functional tricuspid regurgitation of various severities. Correction of mitral valve disease may result in recovery and shrinkage of RV size and improvement of its inlet function, and hence reduction of tricuspid regurgitation severity [47, 48]. In patients with long standing pulmonary hypertension, right ventricular dysfunction and tricuspid regurgitation might remain well established and irreversible [49, 50]. Therefore, it is important to detect increases in right ventricular afterload as early as possible and optimize patients' management to avoid such drastic complications. All patients with left heart valve disease tend to develop a significant drop in RV systolic inlet excursion, tricuspid annular plane systolic excursion (TAPSE) after operative repair/replacement of the valve [51]. The exact underlying explanation behind this phenomenon is not clearly determined yet. Possible explanation for this effect could be due to pericardiectomy with loss of lubricating surface at the anterior surface of the heart or ischaemic damage due to poor RV myocardial preservation during surgery as well as right atrial damage due to placement of bypass cannulae [52]. It has been shown that the size of the right coronary artery (RCA) remain normal in patients with severe aortic valve disease, but dilates in those with mitral valve disease, indicating that

secondary pulmonary hypertension is associated with right ventricular hypertrophy and enlargement of the RCA [36, 37].

Effect of left ventricular diseases on the right ventricle

In patients with restrictive left ventricular physiology, the raised left atrial pressure is transmitted to the right side via the pulmonary circulation causing an increase in pulmonary pressure and RV afterload. Furthermore, the raised left sided atrio-ventricular pressure gradient in early diastole is transmitted to the right side across the interventricular septum which results in suppressed early diastolic right ventricular filling due to high early diastolic intracavitary tension. These disturbances have been shown to reverse with successful offloading of the left atrium and normalisation of left sided pressures [53].

Myocardial blood flow and the right heart

Similar to the left ventricle, maintaining the coronary flow to the RV myocardium is crucial, particularly when RV systolic pressure is raised. For instance, in pulmonary hypertension, where RCA pressure may be increased or remained unchanged, there is an increase in oxygen demand by the myocardium. Since RV perfusion occurs during both diastole and systole, the systolic component is reduced as a result of the raised chamber pressures [54, 55]. Acute RCA occlusion proximal to the RV branch often results in RV free wall dysfunction and in multi-vessel coronary artery disease there is significant ischaemic long axis dysfunction with stress which seems to affect the cardiac output [56]. The long lasting ischaemic right ventricle becomes stiff, dilated and volume dependent which contributes to RV dysfunction. Patients with RV infarction commonly respond positively to volume treatment and early reperfusion enhances recovery of right ventricular performance and improves clinical outcome and survival [57].

Effect of pulmonary diseases on the right heart

Pulmonary diseases may cause an increase in pulmonary vascular resistance (PVR) as well as pulmonary artery pressures. For example, patients with chronic obstructive pulmonary disease (COPD) have a wide range of raised resting pulmonary pressures and several grades of RV dysfunction have been reported in these cases [58-60]. Moreover, depressed RV function may be found in these patients during exercise [61]. Previous literature has shown that in patients

with cystic fibrosis, there is a fall in long axis function [62] and RV diastolic dysfunction has been found in those with COPD and pulmonary embolism [63].

IV. Ventricular interaction

Ventricular interaction is mediated through three mechanisms:

- Pulmonary circulation with changes in right ventricular loading conditions.
- Geometry and motion of the interventricular septum, e.g. by common myocardial fibres.
- Pericardial constraint.

In normal hearts, the interventricular septum is shared by both the right and left ventricles and is known to function as part of the left ventricle. In a study of Hoffman et al. [64], they showed that left ventricular contraction contributed 24% of its own stroke work to the generation of right ventricular stroke work via the interventricular septum and in pulmonary hypertension, the contribution is increased to 35%. In circumstances such as tricuspid regurgitation, atrial or ventricular septal defects, the RV becomes volume overloaded and in pulmonary hypertension it becomes pressure overloaded and as a result the septal motion is reversed and the septum functions as part of the right ventricle in order to maintain the stroke volume [65]. Furthermore, the same pattern of septal dysfunction occurs after heart surgery, although to a much lesser extent, and this is probably to maintain the stroke volume of the right heart. The septum also transmits pressures between the two cavities. Patients with raised left ventricular end-diastolic pressure may present with a dominant 'a' wave in the jugular venous pressure which reflects the increase in left sided end diastolic pressures, transmitted to the right side across the septum [65]. Similarly, patients with pericardial constriction show pressure equalization between the chambers, through a similar mechanism. Likewise, patients with dyssynchronous septum due to pressure or volume overloaded RV present with suppressed left ventricular early diastolic filling component as a result of the transmitted high early diastolic tension from the right ventricle [66]. Ventricular interaction through the interventricular septum was reported to be less important than interaction through the pulmonary circulation but appears to be of great importance for the balance of the right and left cardiac output [67]. The fact that the right and left ventricles are both enclosed within the pericardium suggest that there is potential interaction between the left and right ventricles through changes in intra-pericardial space pressures. Right ventricular volume overload and dilatation of the right heart causes an increase

in intrapericardial pressure, reducing venous return, cardiac output and if not promptly managed will affect left ventricular function [68]. Furthermore, in rapid accumulation of pericardial effusion the intrapericardial pressure is increased and results in RV phasic filling and ejection, with respiration, being predominant during inspiration. As a result, if not managed quickly, this effect could lead to reciprocal left sided behaviour during expiration. The same could apply to patients with large pleural effusion and those with end-stage pulmonary disease [69]. Ventricular interaction, via the pericardial space is most effective in patients with acute rise in intra pericardial pressures e.g. fluid accumulation or acute deterioration of ventricular function and cavity enlargement.

V. Assessment of right heart function

Accurate quantitative evaluation of RV function has remained an elusive clinical challenge. Most investigators attribute the difficulties in finding a reproducible method for assessing RV function due to its complex structural geometry. Magnetic resonance imaging (MRI) known as the gold standard has been extensively validated and is known to give accurate estimates of RV volume and ejection fraction [70, 71] as well as any evidence for RV apical fibrosis of apical fatty infiltration. However it is expensive, of limited availability and is not feasible in heart failure patients, commonly seen in our daily practice, with implantable devices. In addition, most patients with heart failure and fluid retention find it difficult to lie flat for significant length of time in a clostrophobic tube. However, MRI is of great value particularly in patients with complex congenital heart disease. The use of radionuclide angiography requires injection of radioactive agents and has a low spatial resolution. This technique suffers from attenuation artifacts, and differentiation between the RV and right atrium may be difficult [72-74]. Moreover, contrast angiography is invasive and requires contrast injection in potentially haemodynamically unstable patients. First-pass ventriculography has been used historically to assess RV ejection fraction but RV volumes cannot be assessed by this method. With the introduction of single-photon emission computed tomography (SPECT), used with blood pool tracers, both assessment of RV ejection fraction and volumes were made possible [75] at the expense of significant radiation. Echocardiographic measurements of size and estimates of function of the left ventricle are widely used clinically and are known to be of diagnostic as well as prognostic importance in patients with cardiac disease. However, assessment of the right

heart using echocardiography is challenging due to the complex anatomy as well as the heavy trabeculations which make measurement of RV volumes difficult.

VI. Echocardiographic techniques for assessing RV

M-mode echocardiography

A simple and very attractive tool for measuring systolic long axis motion of the RV free wall or TAPSE is the two dimensional guided M-mode [76, 77] which has been shown to correlate with ejection fraction derived by radionuclide angiography [78]. Moreover, it has been demonstrated to be valuable in ischaemic heart disease and cardiomyopathy [53]. The main limitation of this method is that it only represents the inflow segments, thus excluding the RV outflow tract and septal contribution to the overall function of the right heart. Furthermore, in patients with dilated cavity and volume overloaded right ventricle, TAPSE can erroneously overestimate right ventricular function. Additional measurements of the RVOT such as the fractional shortening, adds great value to the overall performance of the RV and has been found to correlate better with pulmonary artery systolic pressure (PASP) compared to long axis [79]. Figure 4 A and B show the measurements of RVOT fractional shortening and TAPSE.

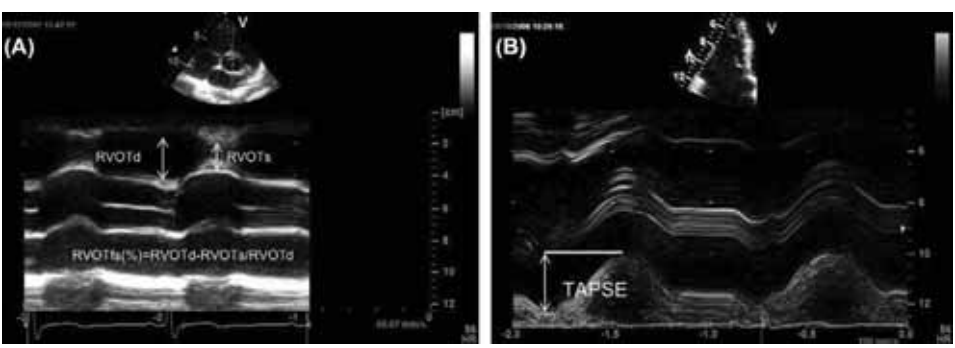

Figure 4. Measurement of RVOT fractional shortening (fs%, panel A and TAPSE, panel B. $RVOT_d$: RVOT diastolic diameter; $RVOT_s$: RVOT systolic diameter

Two dimensional echocardiography

Two-dimensional echocardiography (2DE) remains the most widely available technique, but the complex and three dimensional structure of the RV as well as its heavy trabeculations make the measurement of RV volume difficult. Consequently, evaluation of the RV by 2DE is most commonly qualitative rather than quantitative and this is of limited value in the assessment of the right heart function over time, and in comparing it with MRI volume measurements. Figure 5 A and B show two 2D echocardiographic views, inflow and outflow tracts, which can be used to assess RV function.

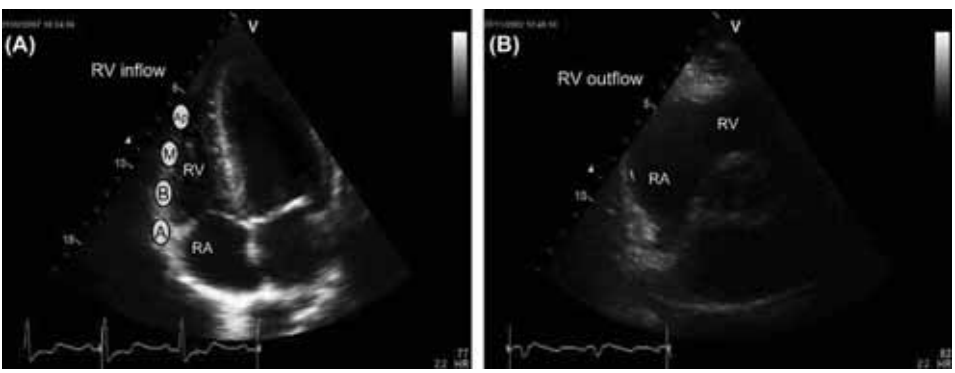

Figure 5. Panel A: The RV viewed from apical four-chamber view with the RA (right atrium) and the inflow tract of the RV. Panel B: The RV is viewed from parasternal short axis view with RV outflow tract visualised. (A) - annular level; (B) - basal level; (M) - mid level; (Ap) - apical level.

One useful method used in clinical practice to calculate volume and ejection fraction is the Simpson's formula which is based on mathematical assumptions of RV geometry, therefore subject to inaccuracies. Furthermore, right ventricular area can be measured from the apical views and the calculated area change which reflects global and regional wall motion can be measured manually and with edge detection, from the RV end-diastolic and end-systolic areas [21, 80, 81]. From the subcostal view, pericardial effusion can be visualised as well as its effect on the RV free wall and from the same view, measuring the diameter of the IVC and the degree of collapsibility during normal breathing or sniff test, right atrial pressure can be estimated. Estimation of RAP is an ongoing topic of discussion and several measures [29] as well as a fixed

value of 7 or 10 mmHg in patients without right heart failure has been proposed [82]. However, inferior vena cava diameter and collapsibility is probably the most commonly used now [83].

Spectral Doppler echocardiography

The peak retrograde trans-tricuspid pressure drop can be obtained by measuring the peak tricuspid regurgitant velocity using continuous wave (CW) Doppler (Figure 6). The pressure drop or gradient ΔP is calculated from the flow velocity (V) using the modified Bernoulli formula, $\Delta P = 4V^2$. The pressure drop is clinically taken as a good estimate of peak systolic pulmonary artery pressure. The trans-pulmonary valve flow can be obtained using Pulse-wave (PW) Doppler with the sample placed proximal to the pulmonary leaflets and RV filling velocities or tricuspid inflow, consisting of early (E) and late filling components (A), with the sample volume placed at the tips of the tricuspid valve leaflets. From these two Doppler waveforms, IVCT, IVRT, pulmonary ejection time (ET) as well as filling time (FT) can all be measured accordingly (Figure 7). A new method to assess overall RV function is Tei or myocardial performance index (MPI). This can be achieved by dividing the total isovolumic time (the sum of the isovolumic contraction and isovolumic relaxation) by the pulmonary ejection time. This index has been found to correlate with pulmonary pressures [84] and can be used for early detection of RV dysfunction in different diseases [85, 86]. The advantage of using this method is that it is reproducible and it avoids the geometric assumptions and limitations of the complex RV geometry. Its main limitation is with increased right atrial pressure, MPI falls due to shortened IVRT [43]. Moreover, it is unreliable when RV ejection time is measured with differing R-R intervals, as in atrial fibrillation. Right atrial filling properties can be assessed from the hepatic venous flow. Finally, relative pulmonary pre-ejection time to that of aortic pre-ejection time reflects the degree of ventricular dyssynchrony.

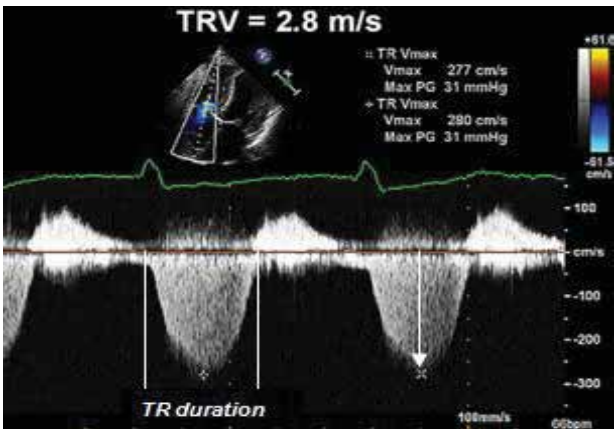

Figure 6. Measurement of peak tricuspid regurgitant velocity (TRV) and TR duration.

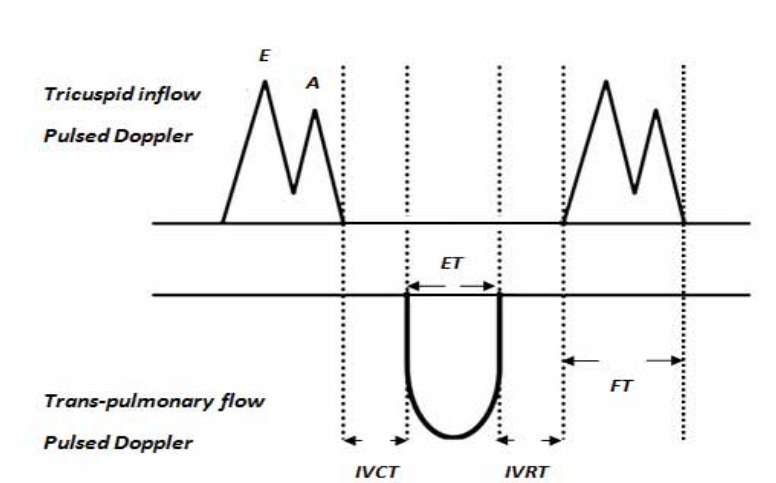

Figure 7. Schematic diagram showing E and A filling components as well as measurement of FT, IVCT, ET and IVRT.

Myocardial Doppler tissue imaging

Doppler tissue imaging (DTI) is a robust technique used to assess RV myocardial function by reflecting RV free wall systolic and diastolic myocardial velocities in a reproducible way. This method, is available on most modern ultrasound systems and provide information on myocardial motion throughout the cardiac cycle [87, 88]. DTI detects low velocities with high amplitudes in contrast to spectral pulsed Doppler echocardiography which detects high velocities with low amplitudes. Furthermore, DTI is less preload dependent compared to the traditional pulsed Doppler technique [89]. Longitudinal RV velocities from Doppler tissue imaging are best recorded at positions showed above in figure 5A, i.e. at positions A, B and M. Pulsed DTI which has a high temporal resolution is simple and more robust to use [90]. The main downfall of this technique is poor spatial resolution due to movement of the heart, whilst the sample volume is fixed and only registers tricuspid annulus motion. It is also limited in measuring apical velocities from the apical long axis projection. One-dimensional strain from colour-coded DTI is an alternative approach of myocardial motion and can be used off-line, therefore suitable during exercise and stress echocardiography. However, it only provides mean values compared to pulsed DTI which, on the other hand, provides peak velocities. The limitation of colour DTI is the lower temporal resolution, but a frame rate above 100 f/s is considered acceptable for measuring time intervals [91]. Using pulsed or colour DTI the systolic (s'), early diastolic (e') and late atrial diastolic (a') velocities can reasonably be measured as well as IVCT, IVRT and ET (figure 8).

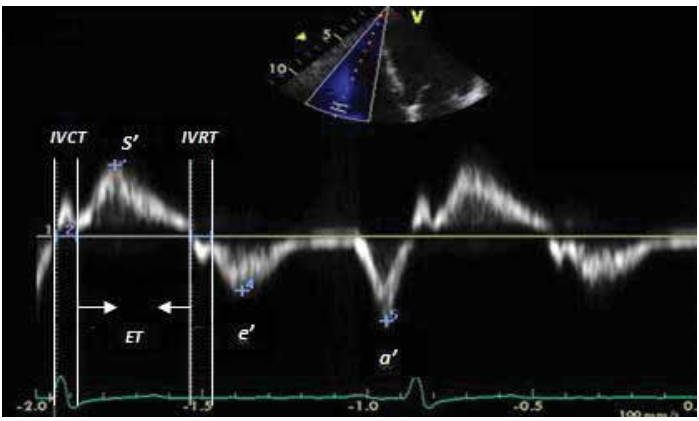

Figure 8. Pulsed DTI showing measurement of s', e', a', IVCT, IVRT and ET)

<u>Two-dimensional strain and strain rate (Speckle tracking)</u>

Strain is defined as the percentage change in myocardial deformation and its derivative, strain rate represents the rate of change of deformation of a myocardium segment over time. Strain and strain rate imaging are used to measure regional and global contractile function using frame by frame tracking of unique speckles in the myocardium. This technique has been validated by ultrasonomicrometry in the longitudinal direction and rotation and it has been widely applied to the LV and most recently used in the assessment of RV in pulmonary hypertension [92]. Its main advantage is that it is angle independent and it can track in two or even three dimensions. Furthermore, it provides segmental as well as global assessment of the myocardium and it possesses an improved signal to noise ratio. On the other hand, the main disadvantage is that there is a lack of normal range for segmental and global measurements. Speckle tracking imaging depends very much on the image quality and drop-outs and reverberations can affect tracking as well as too low or high frame rates. A frame rate between 50 to 80 frames per second is considered ideal for this technique [92, 93].

Real-time 3D echocardiography

Three dimensional echocardiography (3DE) has been developed for the last 15 years and ventricular volume, mass and function can all be accurately assessed as well as a more complete view of the valves can be obtained using such technique. The contrast resolution and penetration have been improved with the newly developed matrix array transducer, consisting of 3,000 firing elements, which is part of the third generation echocardiographic machines. 3D echocardiography has the potential advantage in determining RV volumes and image reconstruction can be performed both off line and also on-line [94-96]. Moreover, 3DE overcomes the geometric limitations of 2D techniques, potentially allowing volume assessment without the use of any geometrical assumption. 3DE overcomes some of the disadvantages of cardiac magnetic resonance (CMR) as it can routinely be used for serial imaging, particularly at the bed-side. On the other hand, 3D echocardiography has a limitation with respect to data acquisition in patients with arrhythmias, including atrial fibrillation and frequent extra-systoles, because acquisition of 5 consecutive stable heart beats is necessary for image reconstruction. The endocardial definition is sometimes difficult to discern in the RV, assessed by 3DE, owing to artifacts and the abundant aberrant papillary muscles. The poor lateral resolution in right ventricular cavity dilatation adds to the limitation of using 3DE to assess RV.

VII. Assessment of pulmonary hypertension

Estimation of peak and mean pulmonary artery systolic pressure

Pulmonary hypertension is considered when PASP exceeds 36 mmHg [97] or mean pulmonary artery pressure (MPAP) exceeding 25mmHg [98]. PASP can be assessed invasively by right heart catheterisation (RHC) in order to obtain direct measurement of right sided pressure. However, Doppler Echocardiography has now made it possible to measure such pressures non-invasively [98]. This can be achieved by measuring the peak tricuspid regurgitant velocity obtained by continuous wave Doppler and applying the equation below:

$PASP = 4 \times (\text{peak TR velocity})^2 + RAP$

The above technique has been shown to correlate with peak pulmonary artery pressure, obtained invasively [82]. It is important to note that determination of pulmonary artery (PA) pressure by Doppler echocardiography relies on the variability of right atrial pressure rather

than direct measurement of PA systolic pressure. However, a rise in RAP, due to significant tricuspid regurgitation or a stiff ventricle, can result in underestimation of the retrograde pressure drop across the tricuspid valve. The mean pulmonary artery pressure can be estimated using the following equations below, from (1) PASP, (2) from the diastolic retrograde pressure drop across the pulmonary valve, which can be obtained from the pulmonary regurgitation (PR) CW Doppler velocities and which has been shown to correlate with invasive measurements [99] and (3) pulmonary artery acceleration time (PAcT) which is measured from the onset to peak RV ejection spectral Doppler signal.

*(1) MPAP = PASP *0.61+2, [100].*
(2) MPAP = $4*PR_{edpd^2}$ + RAP, where edpd = early diastole peak pressure drop, [101, 102].
(3) MPAP = 79-0.45(PAcT) [103, 104]*

It has been found before that a value of PAcT of less than 105 ms is suggestive of pulmonary hypertension [105, 106]. Prolonged isovolumic relaxation time measured from pulsed tissue Doppler imaging (> 75ms corrected to heart rate) accurately identified patients with PASP > 40mmHg, a marker that has proved the best in predicting patients with pulmonary hypertension [107, 108].

Pulmonary vascular resistance

In severe cardiac failure and hyperkinetic circulation, estimation of PVR is usually recommended to avoid any possible errors in assessing the degree of PH [109]. Below are two equations which have been developed over the years to calculate PVR and a value exceeding 3 woods units (WU) is considered abnormal.

*(1) PVR = TR_{pv}/PA VTI*10+0.61, [110].*
pv = peak velocity and PA VTI = pulmonary artery velocity time integral.

(2) PVR = (MPAPecho-PCWP) /CO, [111]
PCWP (pulmonary capillary wedge pressure) was estimated as 10mmHg. The stroke volume (SV) was calculated using the equation: 0.78 x (LVOT diameter) ^{2} x (LVOT velocity time integral) [112]. Cardiac output (CO) was calculated as the stroke volume x heart rate.

The main limitation of Lindqvist et al. equation is the accurate estimation of PCWP, which reflects left atrial pressure, in patients with raised pre-capillary pressures.

One dimensional strain from colour-coded DTI has been shown to be modestly useful in estimating PVR [113] and also to assess the dyssynchrony between the RV and septal segment being shown to determine disease severity [114]. Moreover, myocardial strain and strain rate have been found to be related to the pulmonary pressures and PVR and also to patients' exercise capacity assessed by 6 minutes walk distance (6MWT) [115].

Eccentricity index

Eccentricity index is measured as the ratio of the minor axis of the LV parallel to the septum, to the minor-axis perpendicular to the septum. This index is measured at end-diastole and end-systole. In a purely pressure-loaded RV, there is flattening of the interventricular septum in end-systole, which results in a D-shaped left ventricle, consistent with significant pulmonary hypertension. When the RV enlarges the LV decreases in volume giving an abnormal eccentricity index, i.e. the antero-posterior dimension becomes larger than the septo-lateral dimension which makes the LV cavity D-shaped. LV diastolic function is altered by such abnormal shape as long as myocardial function is preserved [116], which is shown by Doppler as reduced E/A ratio, prolonged deceleration and isovolumic relaxation time.

AIMS AND OBJECTIVES

The aim and objectives of this thesis was to conduct the following studies in an attempt to provide answers for a number of outstanding clinical questions.

1. Differential right ventricular regional function and the effect of pulmonary hypertension: 3D echo study.

It is known that right ventricular function is an integral part of the overall cardiac function having to deliver an optimum stroke volume to the left heart. As described in the introduction section various components of RV cavity, including the inflow, apical and outflow compartments contribute to its overall systolic function. Anatomical studies have demonstrated clear differences between the three RV compartments, not only in their orientation but also myocardial fibre architecture [7, 11, 117-119]. This fact justifies considering the three compartments in detail when describing overall RV function. The three dimensional nature and complex anatomy of the RV make 3D echocardiography and MRI ideal tools for assessing its size and function [120]. Echocardiographic 3D studies have shown RV cavity to be globally impaired in various diseases including pulmonary hypertension. We aimed in this study to assess the normal differential function of the three compartments of the RV and determine their response to left ventricular (LV) failure with and without secondary PH. Furthermore, we aimed to identify the exact determinants of RV peak ejection.

2. Organised right ventricular remodelling in aortic stenosis even after valve replacement

It is known that severe aortic stenosis (AS) causes hypertrophic response of the myocardium due to left ventricular pressure overload. Aortic valve replacement (AVR) results in LV mass regression and improved, even if partially, systolic and diastolic function over the few months after surgery [121-123]. However, the impact of critical AS and AVR on global and segmental right ventricular function remains undetermined. RV function has been shown to fall significantly after cardiac surgery, AVR and coronary bypass [124, 125], and to be the main predictor of exercise capacity after surgery and in heart failure [78, 126-128]. It has been shown that exercise capacity is subnormal after AVR for AS, irrespective of LV ejection fraction [129]. Also, although AVR normalises resting LV longitudinal function, the residual compromised

myocardial function reserve remains an exercise limiting step, irrespective of post-operative closure of the pericardium, [129]. The aim of this study was to assess the pattern and extent of regional RV disturbances in patients with severe AS and its mid-term response to AVR, which could explain the limitation of exercise.

3. Global and regional right ventricular disturbances in patients with pulmonary hypertension and normal left ventricular function

Pulmonary hypertension (PH) as previously discussed, is a serious clinical condition which is known to be progressive and to result in significant damage to the right heart function. PH which imposes pressure overload on the RV, through elevated pulmonary artery pressure can cause premature death in severe cases [130]. It is known that long standing and severe PH can result in intractable and potentially irreversible RV damage, even after lung transplantation [131]. Recent advances have lead to improvement in therapy for certain groups of patients as medical treatment of pre-capillary PH (pulmonary arterial hypertension (PAH) by endothelin receptor antagonists, PDE5 inhibitors and prostacyclins resulted in significant fall in pulmonary resistance but questionable recovery of RV function [132]. The aim of this study was to assess the extent of global and regional RV dysfunction in a group of PH patients, of different aetiologies, and normal left ventricular function.

SUBJECTS AND METHODS

I. Study populations

Study 1

Forty five individuals with good acoustic window underwent two dimensional, and three dimensional, echocardiographic examination, 16 of whom served as controls (age 50 ± 8 years, 9 males) had no left or right heart abnormalities based on conventional echocardiographic, electrocardiographic or history of cardiovascular disease. The remaining 29 patients had known heart failure due to ischaemic heart disease, based on clinical history and examination, coronary angiogram and 2D echocardiographic evidence for LV dysfunction due to previous myocardial infarction. Patients were divided into two groups, Group 1 ischaemic (N = 15) (age 63 ±15 years, 12 males) and Group 2 ischaemic with PH (N = 14) (age 72 ± 14 years, 9 males). No patient had COPD, RV infarction or recent coronary revascularisation procedure, for at least one year prior to the study. The research was conducted with the approval of the ethics committee of the Royal Brompton and National Heart and Lung Institute, United Kingdom.

Study 2

We studied 28 patients (age 63 ± 11 years, 14 males) with severe aortic stenosis (AS) who underwent surgical AVR, at the Heart Centre of Umeå University hospital, using Doppler echocardiography the day before AVR and again 6 months after surgery as part of the postoperative follow up protocol of the centre. The criteria for severe AS, were an aortic valve area of ≤ 1.0 cm^2 and/or a mean transvalvular gradient ≥ 40 mmHg. All patients underwent cardiac catheterisation before surgery to exclude high grade lesions, > 50% narrowing, in one or more of the epicardial coronary arteries. Blood pressure (GE ergometer, model 900, Ergoline GmbH, Germany) was assessed as part of the clinical evaluation at different stages. No patient had more than mild additional valve disease or surgical procedures such as coronary artery bypass or other valve replacement. Other exclusion criteria were signs of restrictive physiology (E/A < 2, E wave deceleration time <130 ms or isovolumic relaxation time <40 ms), pulmonary hypertension, i.e. PASP greater than 36 mmHg, at rest [97] or chronic obstructive lung disease. Also, patients were excluded if they had impaired left ventricular systolic function (ejection fraction <50%) or very poor quality image of the RV. Patients' data were compared with 20 (age

62 ± 15 years, 7 males) healthy individuals with a structurally normal heart and without history of cardiovascular or systemic disease, recruited from the population of Umeå. Informed consent was obtained from patients and controls to participate in the study, which was approved by the local Ethics Committee of Umeå.

Study 3

We performed a cross-sectional study on 35 patients (age 67 ± 12 years, 13 males) with chronic RV pressure overload referred to the Umeå Heart Centre, Sweden. All patients had been diagnosed with PH, confirmed by history taking, physical examination, Doppler echocardiography and right heart catheterisation. PH was defined as mean pulmonary artery pressure greater than 25 mmHg obtained from RHC [98]. No patient had severe anemia or more than mild- moderate valve regurgitation or significantly raised left atrial pressure (LAP) (E/e'>13) due to severe left ventricular disease that could affect RV geometry and function. Other exclusion criteria were inability to analyze images due to poor quality acquisition of the RV, impaired LV systolic function (EF < 50%), history of RV infarction or congenital heart disease. Patients' data were compared with 20 (age 62 ± 15 years, 7 males) healthy individuals with a structurally normal heart and without history of cardiovascular or systemic disease, recruited from the general population of Umeå. The study protocol was approved by the Regional Ethics Committee of Umeå and all subjects signed an informed consent.

II. Methods and measurements

Techniques used to acquire echocardiograms

Study 1: Echocardiograms were obtained with the patient in the left lateral decubitus position using the Philips Sonos 7500 systems, equipped with s3 and x3 transducers with real-time 3D echocardiography capability for image acquisition. Views and measurements were made according to the recommendations of the American Society of Echocardiography and European Society of Cardiology [133]. All examinations were performed by the same investigator.

Study 2 & 3: Transthoracic Doppler echocardiographic examination was performed using Vivid 7 GE Ultrasound system equipped with a 2.5 MHz transducer, with the subject in the left lateral decubitus position. Standard 2D parasternal and apical views were studied using conventional

methods according to the recommendation of the American Society of Echocardiography and European Association of Echocardiography [133]. Blood flow velocities using pulsed and continuous wave Doppler were also obtained. All recordings were made with a simultaneous superimposed phonocardiogram and electrocardiogram, using a sweep speed of 50 and 100mm/s, as appropriate. Examinations were performed by an experienced operator.

Three-dimensional echocardiography

Full volume ECG-gated 3D datasets were acquired from the apical window. Before data acquisition and in order to obtain the optimum placement of the x3 transducer, live 3D-mode imaging was used. The probe was directed laterally and anteriorly until the RV free wall and apex, including the trabecular part, was clearly displayed in the image sector. Once the correct images were obtained, a full volume 3D of the RV was acquired (3-4 beats) during a brief expiratory breath-hold. To maximise the frame rate during acquisition no harmonic imaging was used throughout. The full volume datasets were saved on the system's hard disk then transferred to a workstation, on a CD, for off-line analysis using commercially available 4D-RV-function software (Tomtec 4D RV Function 1.1, Germany). After loading the dataset, three view planes, derived from the full volume, were displayed on the screen and adjusted to obtain the sagittal, coronal and apical 4-chamber plane (A4Ch). The end-systolic and end-diastolic frames were adjusted automatically by the software. Landmarks were set in the centre of the tricuspid and mitral valve in the sagittal plane. The axis line was then moved to the apical region of the LV in the 4-chamber plane and a landmark was set in the centre of the LV in the sagittal plane. In the 4 chamber view, initial contour started at the tricuspid annulus tracing round the ventricle and finishing at the opposite annulus, excluding the trabecular parts. In the sagittal plane, the endocardial border of the RV was traced and in the coronal view two separate contours were drawn along the endocardial borders and along the border of the apex, starting at the tricuspid annulus to the pulmonary annular area, at the end systolic and end diastolic frames, Figure 9 (A). Based on these contours of the three image planes, the software defined a dynamic tripartite Beutel model. This model is automatically adapted to the endocardial surface of the ventricle. The inflow compartment was created from the tracing in the 4-chamber plane and coronal plane i.e. from the tricuspid annular ring to the proximal trabecular apical border. The apical part was obtained from endocardial contours drawn in the sagittal plane to the apical level but tracing around the trabeculae. The outflow tract compartment was created from the intersection point of the perpendicular axis lines of the inflow and apex, which is located on the RVOT apical

border, to the pulmonary annular area. For better accuracy, the contours were corrected manually, frame by frame, in the 4-chamber plane, during systole and diastole to ensure that it follows the movement of the tricuspid ring throughout, before the reconstruction of the final 4D RV model. Figure 9 (B) shows a sketch of a tripartite RV model. The 4D RV model dataset containing the inflow, outflow and apical region measurements were then exported to a spreadsheet and tripartite graphs showing quantification of volume changes during different phases of the cardiac cycle were then plotted, Figure 10 (A) and (B). The ejection fraction (EF %) of the overall RV cavity was automatically generated by the software. The EF of the inflow, outflow and apex were calculated from Figure 10 (A) by subtracting the minimum volume (end-systolic volume) from the maximum volume (end-diastolic volume) of the respective compartment divided by the end-diastolic volume. The extent of volume change (fall or increase) during different phases of the cardiac cycle was quantified. The rate of change of volume at different points on the volume curves was calculated as the difference between two consecutive volumes divided by the time difference, Figure 10 (A). The values were then plotted against time for the inflow, outflow and apex, Figure 10 (B). The end ejection point was taken as the smallest volume on the volume curves of Figure 10 (A).

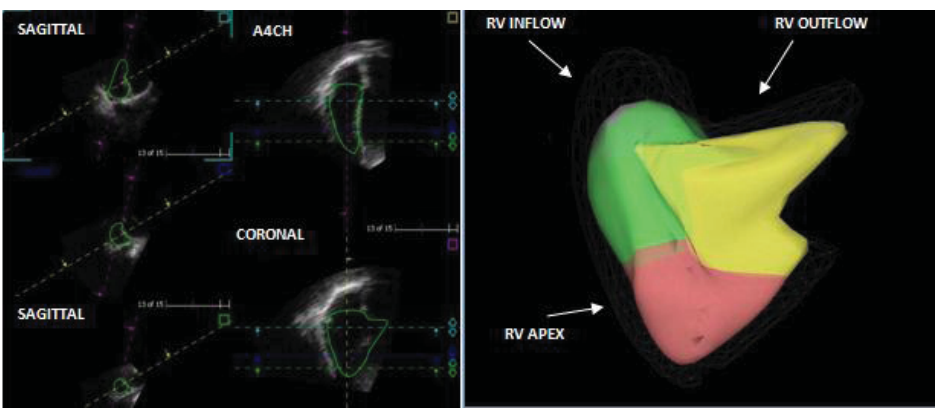

Figure 9. (A) Initial contours drawn on the three planes. (B) Four-dimensional tripartite RV

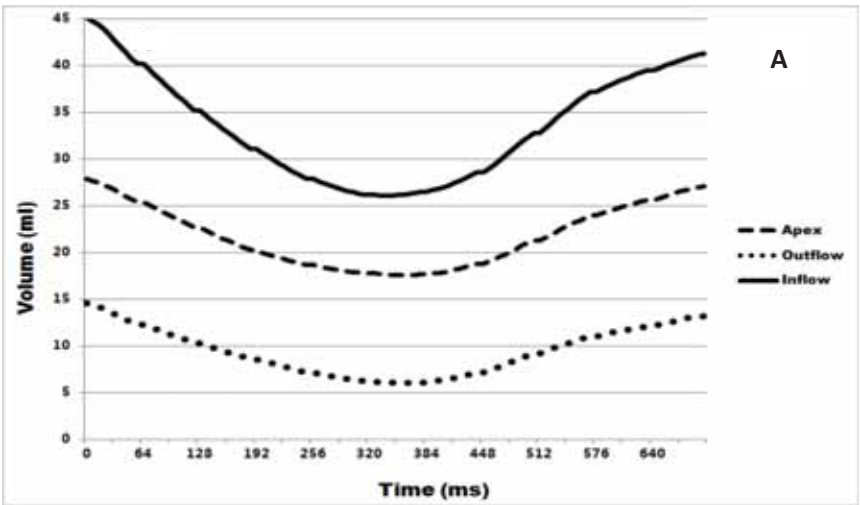

Figure 10. (A): Example of a tripartite graph of one patient; inflow, outflow and apex volume curves.

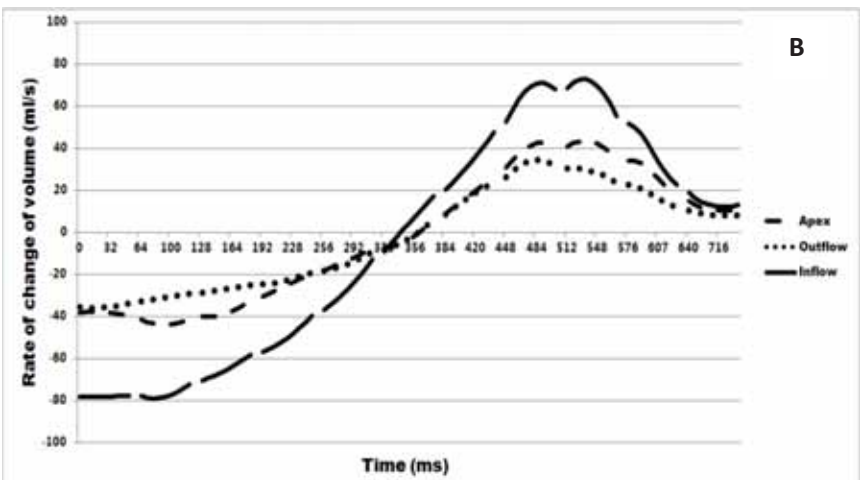

Figure 10. (B): Example of a tripartite graph of one patient; rate of change of volume of the three right ventricular compartments.

Two-dimensional strain rate imaging (Speckle tracking)

Off-line analysis of the RV apical 4-chamber view by speckle tracking echocardiography (STE) for 2D strain rate (SR) measurements was made using the commercially available EchoPac analysis system (GE, version 8.0.1, US). The software is based on real time tracking of natural acoustic markers, present in the ultrasound tissue images, which allows the derivation of 2D strain rate (frame rate = 50 - 54 f/s) by comparing displacement of speckles in relation to one another throughout the cardiac cycle. The inflow compartment of the RV consists of the lateral free wall and septum. The endocardial border of the RV inflow and outflow tract were manually traced and tracked by the software in order to determine the RV longitudinal strain rate (Figure 11 and 12), displacement and velocity of the entire traced contour. The inflow part was divided into three segments; basal, mid-cavity and apical (Figure 11). The region of interest (ROI) of the RV inflow compartment was both the basal and mid-cavity segments of the lateral wall for study 3, but only basal segment was used for study 2. As for the outflow tract compartment (Figure 12), the middle segment was selected in both studies (2&3) and used for analysis in all subjects to ensure consistency of measurements. From the inflow and outflow tract segments the peak systolic SR and peak amplitude of motion were measured. The peak systolic velocity of the basal inflow tract was also recorded using STE. In study 2, from the apical four-chamber view, LV cavity was traced manually from the innermost endocardial edge at end systole and the software automatically defined the longitudinal SR throughout the cardiac cycle. Global systolic longitudinal LV strain rate (GLSRs), which represents the mean systolic longitudinal SR of six segments (basal, middle and apical segments of septal and lateral wall), was measured. The systolic SR was presented as positive value in order to avoid any potential confusion when the linear regression model was performed.

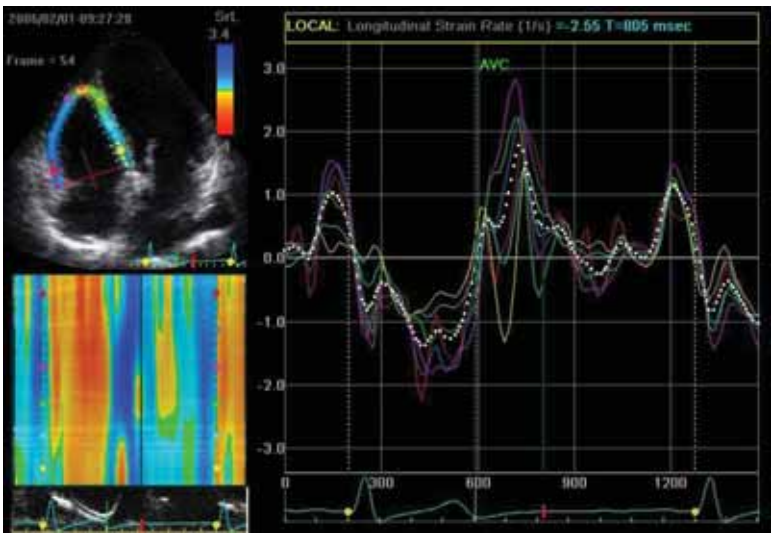

Figure 11. Longitudinal strain rate of the base, mid and apical region of the right ventricle.

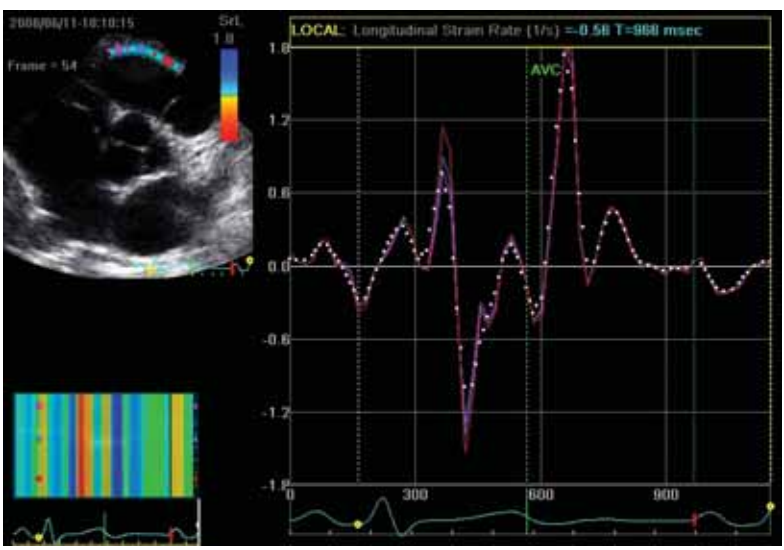

Figure 12. Longitudinal strain rate of the right ventricular outflow tract (RVOT).

2D/M-mode echocardiography

From the parasternal long axis 2D projection, the internal LV end-diastolic and end systolic diameters (LVEDD and LVESD) were measured and in study 2 we also measured the septal and posterior wall thickness (IVST and PWT) at end diastole. From the apical 4-chamber view, LV volumes were measured at end systole (LVESV) and end diastole (LVEDV) and ejection fraction was calculated using bi-plane Simpson's model. From the volume measurements, stroke volume was calculated by subtracting LVESV from LVEDV. LVOT diameter was measured using the leading edge methodology. The left atrium (LA) diameter at end systole was measured as well as LA volume using Simpson's bi-plane model and care was taken to exclude the pulmonary veins during tracing. From the short axis view, RV outflow tract diameters were measured at end diastole and end-systole using the M-mode technique. From the apical 4 chamber view we measured the tricuspid annular diameter using leading edge methodology. From the same view RV long axis motion using the M-mode technique with the cursor positioned at the lateral angle of the annulus, from which TAPSE was measured. Where appropriate, the right atrial minor axis dimension was measured in a plane perpendicular to the long axis of the right atrium, extending from the lateral border of the RA to the inter-atrial septum.

Spectral Doppler and Doppler tissue imaging

LV filling velocities were acquired using pulsed wave (PW) Doppler recording with the sample volume placed at the tips of the mitral valve leaflets and transmitral E and A diastolic velocities were measured as well as E/A ratio calculated. Pulsed Doppler tissue imaging was also used to record LV myocardial velocities with the sample volume placed at the base of the lateral wall. The ratio (E/e') of transmitral early diastolic velocities, to that from DTI was calculated. Semi-quantitative mitral regurgitation, where appropriate, was assessed by the extent of regurgitant jet area as a percentage of the left atrial area using Doppler imaging with colour flow mapping. LVOT velocity time integral (VTI) was also measured from the pulsed wave recording of outflow tract velocities. From the Doppler measurements, stroke volume was also calculated from the equation previously described, i.e. 0.78 x (LVOT diameter) ^{2} x (LVOT VTI). Cardiac output was calculated as the product of stroke volume and heart rate, as previously described. Continuous wave (CW) Doppler recording across the aortic valve was acquired to obtain the peak and mean transvalvular pressure drop in study 2.

RV filling was recorded with the pulsed wave Doppler sample volume positioned at the tips of the tricuspid valve leaflets. The onset of diastole was taken from the end-ejection marked as the onset of the pulmonary component of the second heart sound (P2) of the superimposed phonocardiogram. The onset of RV filling was taken as the onset of early diastolic filling after P2. Tricuspid regurgitation was obtained using the continuous wave Doppler with the cursor placed across the tricuspid valve leaflets and the modified Bernoulli equation was used to estimate the right ventricular - right atrial peak pressure drop. PASP was estimated using the equation 4 x (peak TR velocity)^2 + RAP as previously described. The PW Doppler of the trans-pulmonary flow or RV ejection velocities was also recorded with the sample volume placed 1 cm distal to the pulmonary valve leaflets [134-136] and end ejection was taken as the pulmonary valve closure artefact. Pulmonary ejection acceleration (PAc) was measured from the onset to peak ejection using the provided callipers.

M-mode/Doppler timing measurements

All time measurements were taken with respect to the Q-wave of the superimposed ECG and were corrected to heart rate.

From the M-mode recording, the time to onset and peak shortening of the basal segment were measured. From spectral Doppler recordings, we measured the time to onset of RV filling and total filling time as the total duration of filling, from its onset to its end, as shown in Figure 7. Duration of TR was measured from its onset in early systole to its end in early diastole, as shown in Figure 6. We also measured 1) IVCT, between the onset of q-wave of the ECG and the onset of RV ejection (Figure 7); 2) time to peak RV ejection; 3) time to end RV ejection; and 4) IVRT, between RV end ejection and onset of filling (Figure 7). The acceleration time (AccT) of the pulmonary artery was taken as the time interval between the onset and peak RV ejection and deceleration time (DeccT) as the time interval between peak and end-ejection. We also measured ejection time (ET) by subtracting the time to onset from time to end of ejection and total isovolumic time was obtained by subtracting ET from time to onset of RV filling. RV myocardial performance index (MPI) was calculated by dividing total isovolumic time by ET.

Strain rate timing measurements

From the inflow and outflow tract STE recordings, we measured the time to peak amplitude of segmental shortening and the time to peak systolic SR with respect to the onset of the Q wave of

the superimposed ECG. We used the superimposed phonocardiogram to determine the closure time of the pulmonary and aortic valve, which reflects end-systole of RV and LV, respectively.

Three dimensional timing measurements

The four time intervals IVCT, IVRT, AccT and DeccT, measured from PW spectral Doppler recordings were superimposed and adjusted on the 3D volume curves of Figure 10 A&B and regional volume changes at inflow, outflow and apex were assessed. All time measurements were made from the reference line at 0 ms from the 3D volume curves.

Cardiac catheterisation

All cardiac catheterisations where appropriate were performed by one experienced investigator. An introducer was inserted in a medial cubital vein or in the femoral vein for venous access. A swan-Ganz® Standard thermodilution catheter (Edwards Lifesciences) was used to perform retrograde catheterisation. Mean right atrial pressure, systolic and end-diastolic right ventricular pressure, pulmonary artery systolic, mean and diastolic pressures as well as pulmonary capillary wedge pressure were measured. Blood samples for estimation of oxygen saturation were drawn from the superior and inferior caval veins, right atrium and from the pulmonary and femoral arteries.

Statistical analysis

Simple statistics were used in all three studies using a commercially available statistics program (SPSS 13). Data are presented as mean ± standard deviation or as numbers. A non-parametric Mann-Whitney test was used to compare differences between groups. Pearson's correlations was used to test relationships between variables, such as specific 2D and 3D variables in study 1. In study 2 & 3, univariate correlations between ejection time and SR measurements as well as other variables e.g. LV and RV echocardiographic indices were obtained by using the regression model. In study 2, we included clinical data such as age and systolic blood pressure in our analysis. The variables in the univariate regression model which reached statistical significance were entered into a multiple regression model to determine the independent predictors of time to peak RV ejection. The regression coefficients obtained from the univariate analysis in study 3 were also compared with Spearman correlation. Linear regression analyses were plotted to show

certain relationships where appropriate. In study 1, there was age difference between controls and group 1, controls and group 2. To make variables difference clear, univariate analysis of variance using general linear model was performed with age as a covariate. A Wilcoxon test was used to compare non-parametric variables within each group. Data points were excluded when measurements were not possible due to poor image acquisition. A P value < 0.05 was considered significant.

Reproducibility

Reproducibility of the analysed data were performed by repeating the measurements by the same investigator (intra-observer) and independently by a second experienced investigator (inter-observer) blinded to the results of the initial assessment, from 10 randomly chosen subjects in each study. Inter-observer variability was performed 1 to 2 months after initial assessment. In study 1, the 3D variables used to assess reproducibility were, overall RV EF, end diastolic and systolic volumes, stroke volume and segmental inflow, outflow and apical EF. In study 3 we assessed SR measurements from the tracings around the inflow and outflow tracts of the RV and measuring the time from the onset of Q-wave to peak systolic SR of the base, mid and RVOT. The same technique was used for study 2 with measurement of the time from the onset of Q-wave to peak systolic SR of the base and RVOT only. Coefficient of variation was calculated and presented as the ratio of the standard deviation of the variables to their corresponding mean from the original data set for both study 1 & 2. Bland-Altman comparisons of the variables were also used in study 1. As for study 3, intraclass correlations obtained from the same observer as well as the other independent observer, were presented.

RESULTS

Study 1: Differential right ventricular regional function and the effect of pulmonary hypertension: 3D echo study.

The general characteristics of the three groups (25 patients chosen randomly) are shown in Table 1 below. Left heart failure patients without pulmonary hypertension were classified as group 1 and those with PH as group 2. Also, we found that RV inlet diameter (2D) correlated with end-diastole volume (3D) ($r = 0.69$, $p<0.001$) and TAPSE (2 D) correlated with EF (3D) ($r = 0.71$, $p<0.001$), Figure 13 (A) and (B).

Table 1. *General characteristics of the three groups (25 patients)*

	Controls	Group 1	Group 2	P(1)	P(2)	P(3)
Heart rate, bpm	67 ± 3	68 ± 2	70 ± 2	0.6	0.1	0.1
LVEDD, mm	45 ±9	60 ± 5	62 ± 6	< 0.001	< 0.001	0.07
LVEF %	58 ± 3	36 ±5.8	31 ±4.6	< 0.001	< 0.001	0.13
Mitral regurgitation (patients)		10	10			
Mild		7	2			
Mild-moderate		3	8			
Right ventricular inlet diameter, mm	31 ± 3	40 ± 5	43 ± 3	< 0.001	< 0.001	0.052
TAPSE, cm	2.7±0.2	1.7±0.5	1.4±0.3	< 0.001	< 0.001	0.1
RVSP, mmHg	30 ± 2	31 ±3.2	51 ±6.2	0.4	< 0.001	< 0.001

P (1) = p-value controls vs. Group1; P (2) = p-value Controls vs. Group 2; P (3) = p - value Group 1 vs. Group2; TAPSE = tricuspid annular plane systolic excursion; LVEF = Left ventricular ejection fraction; RVSP = Right ventricular systolic pressure; LVEDD = left ventricular end diastolic diameter.

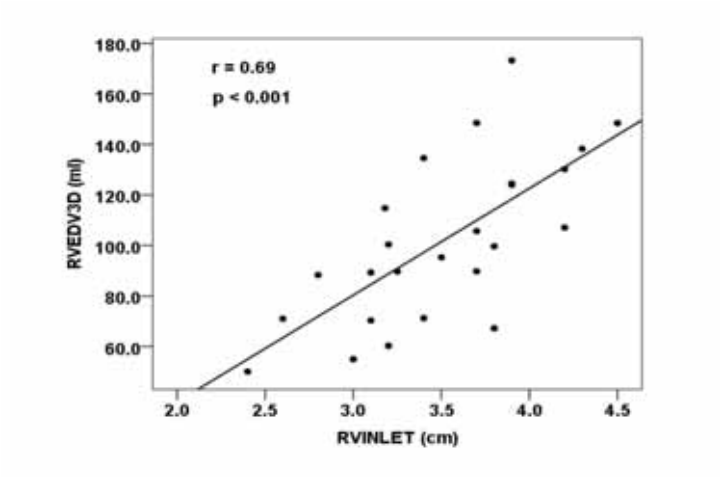

(A)

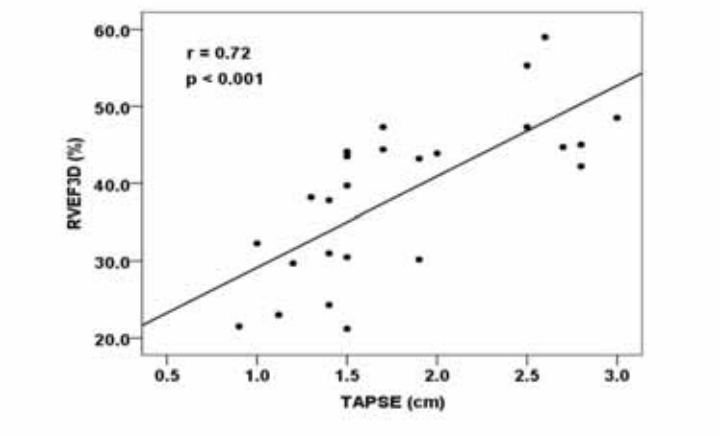

(B)

Figure 13. (A) Correlation between right ventricular end-diastolic volume 3D (RVEDV3D) and RV inlet diameter 2D (RVINLET). (B) Correlation between right ventricular ejection fraction 3D (RVEF3D) and tricuspid annular plane systolic excursion (TAPSE)

RV regional EF and its time relations (Table 2, Figure 14 A and B)

In controls, there was no difference in EF between the inflow and outflow tract compartments, but apical EF was significantly less than both; (inflow $p<0.01$ and outflow $p<0.01$). Group 1 and 2 had increased overall RV end-diastolic and end- systolic volume ($p<0.001$ for both) but overall EF was reduced compared to controls ($p<0.001$ for both). Regional EF was also equally reduced in the two patient groups compared to controls, inflow ($p<0.001$ for both), apical ($p<0.01$ for both) and outflow tract ($p<0.05$ for both). While there was no difference between inflow and outflow tract EF in the two patient groups, the apical EF was less than the two compartments respectively, Group 1 ($p<0.05$ and $p<0.01$) and Group 2 ($p<0.05$ and $p<0.01$) (Figure 14 A). In controls, the inflow compartment reached the minimum volume approximately 20 ms before the outflow tract ($p<0.01$) and before the apex ($p<0.001$). In Group 1, it was only earlier than the apical compartment ($p<0.05$) but not different from the outflow tract (p=NS). In Group 2, there was no time difference between the 3 compartments (p=NS), Figure 14 B.

RV cavity time relations (Table 2)

Compared to controls, IVCT and IVRT were prolonged ($p<0.01$ for both). Pulmonary artery acceleration time was shorter in Group 2 than controls ($p<0.001$) and Group 1 ($p<0.01$).

Events during individual phases of the cardiac cycle (Figure 15 A, B, C, D)

IVCT: In controls, the fall of RV inflow volume was greater than the apex and outflow tract ($p<0.001$ for both). The respective fall of inflow volume in Group 1 was not different from controls, but almost doubled in Group 2 ($p<0.001$).

Acceleration time: The extent of fall of inflow volume in the 2 patient Groups was significantly reduced compared to controls ($p<0.01$ and $p<0.05$, respectively). The fall of apical volume was reduced only in Group 2 ($p<0.05$).

Deceleration time: Only the inflow volume fall was reduced in Group 1 ($p<0.05$) vs. controls. The respective changes in Group 2 were greater than Group 1 ($p<0.01$). Similar findings were seen in the outflow tract ($p<0.01$) in Group 2 when compared to controls.

IVRT: In controls, the fall of inflow volume was double the apical region ($p<0.01$) and 4 times that of the outflow tract ($p<0.001$). These relative differences did not significantly change in Group 1. Respective values in Group 2 were 2.4 times ($p<0.001$) and 3 times ($p<0.001$) those in controls.

Correlation between rate of volume fall and time to peak ejection

In controls, the outflow tract was the only compartment where the rate of volume fall correlated with the time of peak ejection, $r = 0.62$, $p = 0.03$. In Group 1, this relationship was lost and became with the inflow compartment $r = 0.61$, $p = 0.01$. In Group 2, the highest correlation was with the apex $r=0.60$, $p<0.05$, but not with the outflow tract.

Intra-observer and inter-observer variability (Figure 16 (A-D) and Figure 17 (A-D)

For intra-observer reproducibility, the coefficient of variation was EF: 6.0%, EDV: 7.2%, ESV: 8.6%, SV: 9.9%, inflow EF: 3%, outflow EF: 7% and Apex EF: 5%. Respective values for the inter-observer reproducibility were EF: 5.4%, EDV: 3.6%, ESV: 7.6%, and SV: 11.1%, inflow EF: 4%, outflow EF: 6% and Apex EF: 6%.

Table 2. *Echocardiographic tripartite right ventricular parameters*

	Control (n=16)	Group1 (n=15)	Group 2 (n=14)	P (1)	P (2)	P (3)
Age, years	50 ± 7.7	63 ± 14.6	72 ± 14.6	0.01	<0.001	0.07
End diastolic volume, ml	78.6 ± 18.6	109.5 ± 36.0	125.6 ± 30.0	<0.01	<0.001	0.12
End systolic volume, ml	41.2 ± 11.1	74.9 ± 29.4	82.7 ± 25.5	<0.001	<0.001	0.25
Ejection fraction %	47.9 ± 5.8	32.4 ± 8.1	34.7 ± 9.2	<0.001	<0.001	0.75
Ejection fraction (I), %	50.9 ± 7.6	33.1 ± 9.0	36 ± 10.9	<0.001	<0.001	0.66
Ejection fraction (O), %	51.8 ± 9.6	40.5 ± 16.0	41.2 ± 14.2	0.03	0.05	0.92
Ejection fraction (A), %	39.4 ± 8.8	26 ± 8.5	27.8 ± 9.7	0.001	<0.01	0.65
IVCT, ms	71.9 ± 16.9	91.3 ± 23.6	103.6 ± 23.1	0.02	<0.01	0.14
AccT, ms	137.5 ± 15.3	119.3 ± 25.8	92.1 ± 27.8	0.16	0.001	0.01
DeccT, ms	164 ± 22.2	155.3 ± 40.3	177.1 ± 34.3	0.20	0.97	0.21
IVRT, ms	49.7 ± 8.3	69 ± 20.7	73.6 ± 13.4	0.01	0.01	0.76
Rate of volume fall (ml/ms)						
Inflow	– 67.5 ± 21.6	– 51.2 ± 22.1	–79.2 ± 31.1	0.04	0.69	0.01
Outflow	– 19.3 ± 5.4	– 18.9 ± 4.0	–27.6 ± 11.0	0.83	0.06	0.01
Apex	– 28.2 ± 13.9	– 31.3 ± 9.9	– 34.7 ± 10.2	0.33	0.10	0.40

P (1) =p-value Controls vs. Group1; P (2) = p-value Controls vs. Group2; P (3) =p-value Group1 vs. Group2; RV = right ventricle; AccT = acceleration time; IVRT = isovolumic relaxation time; IVCT = isovolumic contraction time; I = inflow; O = outflow; A = apex; DeccT = deceleration time.

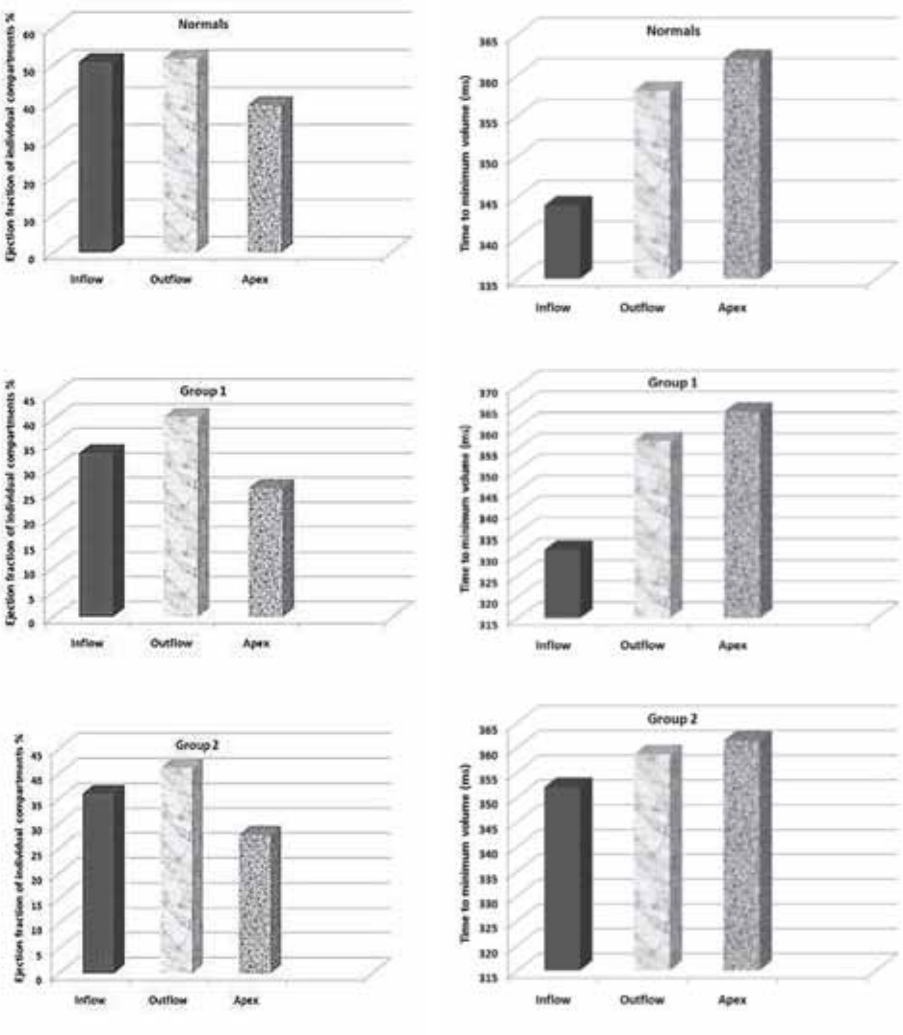

(A) **(B)**

Figure 14. (A) Comparison of ejection fraction of the inflow, outflow and apex in the three patient groups. (B) Comparison of the time interval from the reference line 0 ms to the smallest volume on the 3D volume curves in the three patients groups.

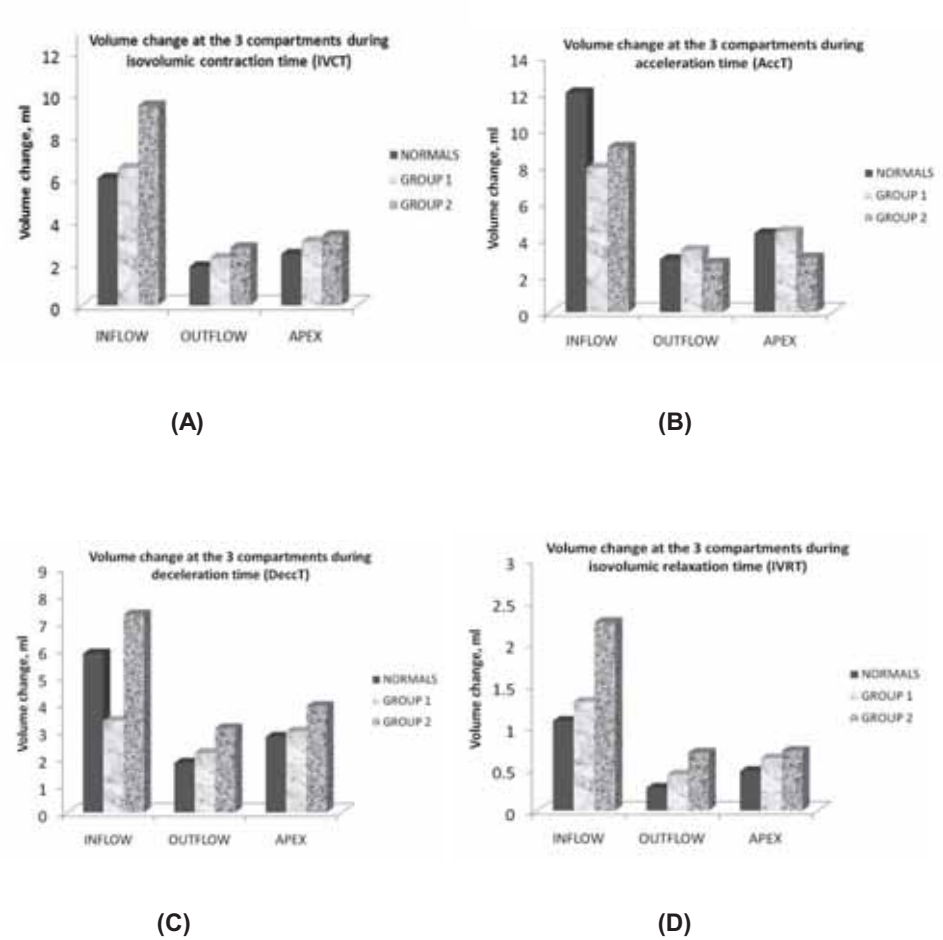

Figure 15. Bar charts comparing 3D volume change in three groups of patients during (A) isovolumic contraction time; (B) acceleration time; (C) deceleration time; (D) isovolumic relaxation time in the three groups of patients.

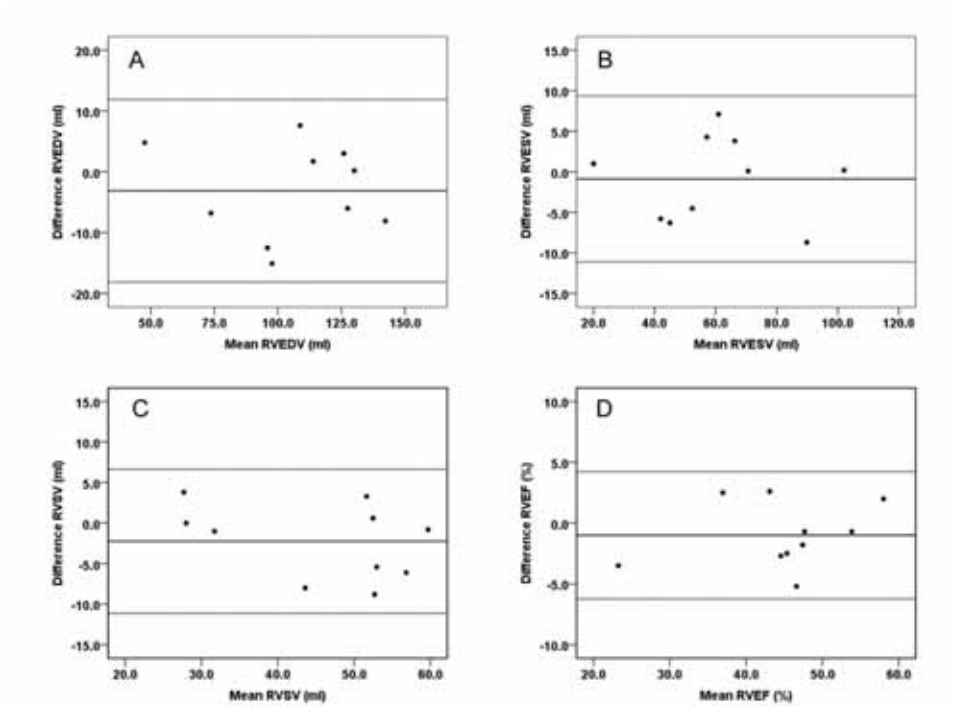

Figure 16 (A-D). Bland-Altman analysis for intravariability. RVEDV: right ventricular end-diastolic volume; RVEF: right ventricular ejection fraction; RVESV: right ventricular end systolic volume; RVSV: right ventricular stroke volume.

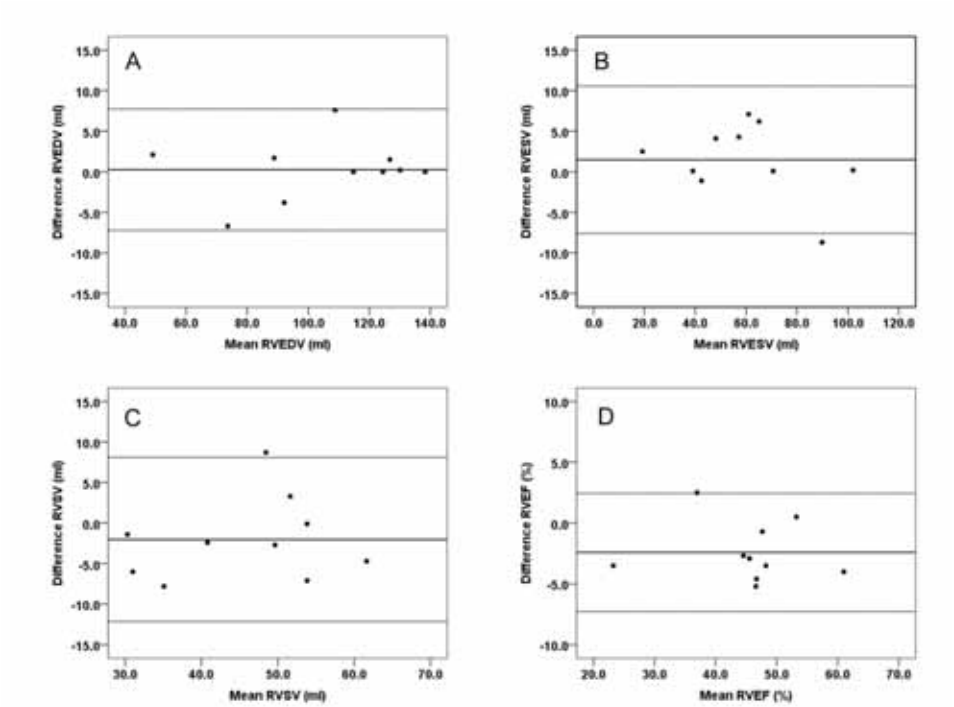

Figure 17 (A-D). Bland-Altman analysis for intervariability. RVEDV: right ventricular end-diastolic volume; RVEF: right ventricular ejection fraction; RVESV: right ventricular end systolic volume; RVSV: right ventricular stroke volume.

Study 2: Organised right ventricular remodelling in aortic stenosis even after valve replacement

LV and RV structure and function (Table 3)

Age and heart rate were comparable between patients and controls. Twelve of the 28 patients had additional systemic hypertension causing a slightly raised systolic blood pressure values with respect to controls ($p<0.01$). Compared to controls, patients had decreased LV end diastolic diameter ($p<0.01$) and ejection fraction ($p<0.001$), with no further change six months after AVR. IVST and PWT were both increased in patients ($p<0.001$ for both) and remained after surgery. LV E/A ratio, LA diameter and CO were not different from controls and remained unchanged after AVR. The tricuspid annulus ($p<0.01$) was dilated pre-operatively as was the RVOT in systole and diastole ($p<0.001$ for both) and all of these measurements remained unchanged after AVR. RA size and PASP were comparable between controls and patients. MPI was increased in pre-op patients ($p<0.05$), when compared to controls and remained unchanged, after surgery.

RV regional, pump timing and global LV function (Table 4)

Compared to controls, there was no difference in RV longitudinal displacement at basal level pre-operatively, but it fell significantly after surgery ($p<0.05$). In contrast, RVOT longitudinal displacement (STE) was exaggerated before surgery ($p<0.001$) and remained unchanged afterwards. RV inlet velocity (STE) and longitudinal SR at the base were all not different from controls before AVR, but significantly reduced after AVR ($p<0.05$ for both). RVOT longitudinal SR was normal before and remained unchanged after AVR. When compared to controls, GLSRs was significantly reduced in patients before surgery ($p<0.001$) and after AVR GLSRs was significantly increased with respect to pre-op values ($p<0.001$).

Timings: Compared to controls, overall RV ejection time was shorter pre-operatively ($p<0.05$) and remained unchanged after surgery. Time to peak systolic SR at base and RVOT were all short pre-operatively ($p<0.05$ and $p<0.01$) and remained unchanged post-operatively. Respective time to peak longitudinal displacement (STE) at basal and RVOT levels were reduced ($p<0.01$ and $p< 0.001$, respectively) and remained short after AVR.

RV segmental vs. cavity function

In controls, CO correlated with peak RVOT displacement (STE) (r= 0.5, p=0.03), but this relationship was lost in patients before (r=0.09, p=0.67) and after surgery (r=0.39, p=0.08). Time to onset of RV filling correlated with TR duration in controls (r=0.7, p < 0.001) and in patients, pre-operatively (r=0.6, p=0.001) and post-operatively (r=0.76, p < 0.001). In controls, the time to peak ejection correlated with the time to peak SR of the RVOT (r= 0.7, p < 0.001), (Figure 18) but not at the basal segment (r=0.19, p=0.4). In addition, it also correlated negatively with RVOT displacement (r= -0.5, p=0.03), SBP (r= -0.45, p=0.046) and PWT (r= -0.45, p=0.048). In contrast, pre-operatively patients' time to peak ejection correlated with the basal time to peak SR (r=0.72, p<0.001) (figure 19) and negatively with MPI (r= -0.42, p=0.04) but not with the RVOT (r=0.1, p=0.62). The same pattern of disturbance remained post-operatively, basal (r=0.71, p<0.001) (figure 20) and RVOT (r=0.08, p=0.7). Furthermore, in patients, time to peak RV ejection correlated with RVOT SR (r= 0.45, p= 0.046) and negatively with age (r= -0.4, p= 0.048) and MPI (r= -0.55, p= 0.005). In the multivariate model, time to peak systolic SR of the RVOT in controls was the only independent predictor of time to peak RV ejection (Beta = 0.63, p=0.004). In patients, time to peak systolic SR at the basal segment (Beta = 0.64, p<0.001) was the strongest independent predictor of time to peak RV ejection, as compared to MPI (Beta = -0.3, p=0.046), pre-operatively. The same applied to post-op results with time to peak SR at base (Beta = 0.61, p<0.001) and MPI (Beta = -0.44, p=0.003).

Table 3. *LV and RV structure and function*

	Controls (n=20)	Pre-op Severe AS (n=28)	Post-op AVR (6months) (n=28)	p(1)	p(2)
Age (years)	62 ±15	63 ± 11	62 ± 11	0.8	0.9
Heart rate (bpm)	63.4 ± 8.9	68.4 ± 9.2	68.6 ± 10	0.1	0.9
SBP (mmHg)	125 ± 6	132 ± 9	133 ± 9.4	0.008	0.6
LVEDD (cm)	5 ± 0.5	4.4 ± 0.4	4.3 ± 0.7	0.001	0.7
LVESD (cm)	3 ± 0.3	2.9 ± 0.4	2.8 ± 0.4	0.6	0.4
LVEF (%)	67 ± 6	58 ± 3	59 ± 4	< 0.001	0.26
IVST (cm)	0.9 ± 0.1	1.17 ± 0.08	1.2 ± 0.1	< 0.001	0.3
PWT (cm)	0.7 ± 0.1	1.12 ± 0.08	1.1 ± 0.1	< 0.001	0.2
E/A (LV)	1.1 ± 0.3	0.9 ± 0.3	1 ± 0.4	0.05	0.05
LA diameter (cm)	3.8 ± 0.5	4 .1 ± 0.7	4.2 ± 0.7	0.27	0.6
CO (l/min)	5.3 ± 1.2	5.1 ± 1	4.9 ±1.1	0.5	0.46
TAD (cm)	3.1 ± 0.3	3.4 ± 0.4	3.5 ± 0.4	0.005	0.2
RVOT EDD (cm)	2.9 ± 0.3	3.3 ± 0.4	3.3 ± 0.3	< 0.001	0.89
RVOT ESD (cm)	1.8 ± 0.2	2.2 ± 0.4	2.2 ± 0.4	< 0.001	0.67
Right atrial size (cm)	0.4 ± 0.1	0.35 ± 0.05	0.3 ± 0.1	0.7	0.8
MPI (RV)	0.3 ± 0.1	0.45 ± 0.26	0.4 ± 0.2	0.04	0.8
PASP (mmHg)	30 ± 3.8	31 ± 3.7	31 ± 3.2	0.4	0.9

LV = left ventricle; LVEF = left ventricular ejection fraction; E/A = early/late diastolic velocity; CO = cardiac output; EDD = End diastolic diameter; ESD = End systolic diameter; RVOT = right ventricular outflow tract; p(1) = p- value controls vs. severe AS; p(2) = p- value severe AS vs. post AVR (6 months); SBP = systolic blood pressure; IVST = interventricular septal thickness; PWT = posterior wall thickness; MPI (RV) = right ventricular myocardial performance index; PASP = peak pulmonary artery pressure; TAD = tricuspid annular diameter; LA = left atrium.

Table 4. *RV regional, pump timing and global LV function*

	Controls (n=20)	Pre-op Severe AS (n =28)	Post -op AVR (6months) (n=28)	p(1)	p(2)
RV (base) longitudinal D, mm	16 ± 3.5	18 ±7	14 ± 5.2	0.4	0.03
RVOT longitudinal D, mm	1.8 ±1.1	3.4 ± 1.4	3.8 ± 2.4	<0.001	0.89
RV inlet velocity, cm/s	9.9 ±1.4	9.8 ± 2	8.4 ± 1.7	0.8	0.008
RV (base) longitudinal SR, (1/s)	1.9 ± 0.5	1.8 ± 0.6	1.5 ±0.5	0.68	0.04
RVOT longitudinal SR, (1/s)	1.6 ± 0.9	1.8 ± 0.8	1.7 ± 0.7	0.6	0.76
GLSRs (LV), (1/s)	0.8 ± 0.1	0.6 ± 0.06	0.9 ± 0.1	<0.001	<0.001
Overall ejection time (PW), (ms/bpm)	6.9 ± 1.2	6 ± 0.92	5.8 ± 1.1	0.017	0.36
TSR at base, (ms/bpm)	3.7± 0.93	3.1 ± 0.86	3.2 ± 0.85	0.04	0.88
TSR at RVOT, (ms/bpm)	3.8 ±0.96	3 ± 0.92	3 ± 0.74	0.003	0.66
TPD at base, (ms/bpm)	6.6 ±1.1	5.4 ±1.3	5.4 ± 1.7	0.004	0.91
TPD at RVOT, (ms/bpm)	6.6 ±1.8	4.5 ± 1.3	4.8 ± 1.7	<0.001	0.58

RV = right ventricle; RVOT = right ventricular outflow tract; STE = Speckle tracking echocardiography; p(1) = p - value controls vs. severe AS; p(2) = p - value severe AS vs. post AVR (6 months); PW = pulse wave spectral Doppler; GLSRs (LV) = global longitudinal left ventricular strain rate; RVOT = right ventricular outflow tract; STE = Speckle tracking echocardiography; base = basal segment; SR: strain rate; D = displacement; TSR: time to peak SR; TPD: time to peak displacement.

Intra-observer and inter-observer variability

For intra-observer variability, the coefficient of variation was: time to peak systolic SR at RV basal: 4.1% and OT: 1.4% segments. Respective values for the inter-observer reproducibility were: time to peak systolic SR at RV basal: 6.6% and OT: 1.6% segments.

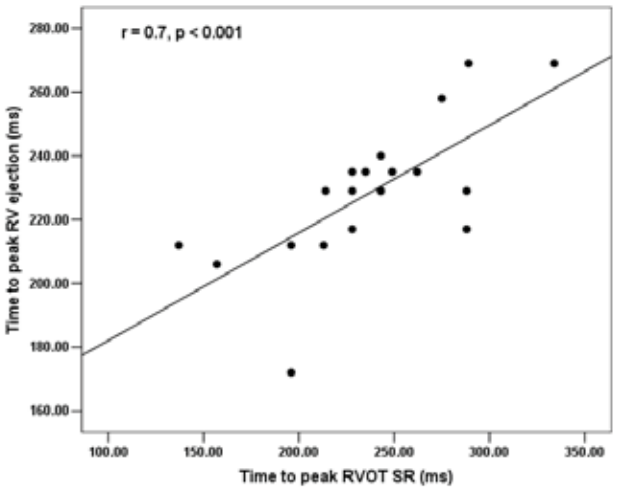

Figure 18. Segmental RVOT correlation with RV ejection in normals

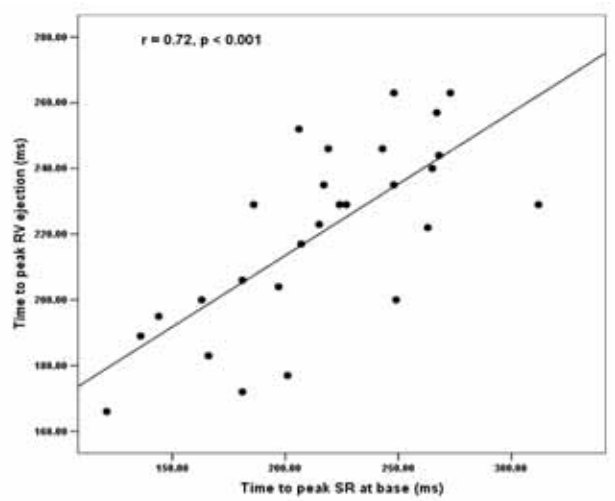

Figure 19. Segmental basal correlation with RV ejection in severe AS patients

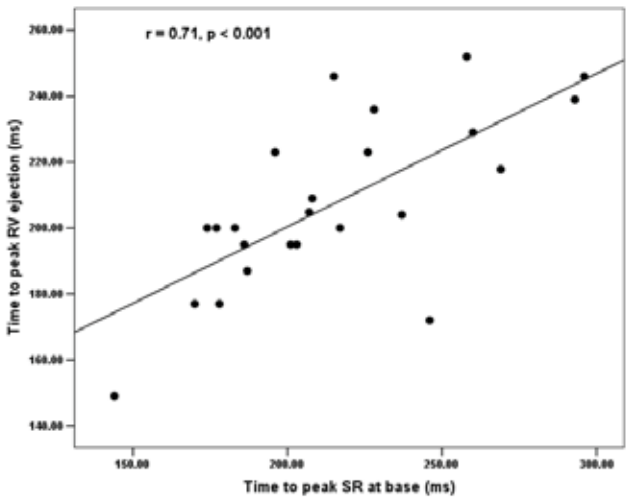

Figure 20. Segmental correlation with RV ejection in six months post-surgery patients

Study 3: Global and regional right ventricular disturbances in patients with pulmonary hypertension and normal left ventricular function

The aetiology of PH is shown in Table 5 below. The 12 lead ECG analysis showed that 50 % of the patients had QRS duration > 100ms.

Table 5. *Clinical characteristics of patients*

Aetiology of PH (n = 35)	Value
Idiopathic pulmonary arterial hypertension (IPAH)	9
Associated pulmonary arterial hypertension (APAH)	14
Pulmonary veno-occlusive disease (PVOD)	2
Chronic thromboembolic pulmonary hypertension (CTEPH)	7
Lung fibrosis	1
Others	2

PH: pulmonary hypertension

LV and RV structure and function (Table 6)

When compared to controls, patients had lower LVEDV (p=0.008), LVEF (p=0.02) but no difference in LA volume (p=0.16). They also had dilated tricuspid annulus (p<0.001) and larger RVOT (p<0.001), higher PAc (p=0.001), reduced TAPSE (p<0.001) and stroke volume (p=0.004) but raised E/e' ratio (p=0.04). RV MPI was significantly higher than controls (p<0.001).

RV myocardial function (Table 7 and 8)

In patients, RV inlet velocity ($p<0.001$) as well as basal and mid-cavity myocardial SR and longitudinal displacement were all reduced ($p<0.001$ for all). The time to onset ($p=0.007$) and peak ($p=0.009$) shortening of the basal segment were reduced as was that to peak basal and mid-cavity systolic SR ($p<0.001$) and peak displacement ($p<0.001$ for both). Respective time measurements of RVOT were also all reduced, ($p=0.007$ and $p<0.001$).

RV filling and ejection (Table 8)

In comparison with controls, patients had shorter filling time ($p=0.03$) and the time to peak ($p=0.001$) and end ($p=0.001$) of RV ejection. TR duration ($p=0.3$) and time to onset of RV filling ($p=0.8$) and to onset of RV ejection ($p=0.5$) were not different.

Relationship between time to peak RV ejection and cardiac function parameters

The univariate regression analysis showed the following: In controls, the time to peak RV ejection correlated with that to peak systolic SR of the OT ($r = 0.7$, $p<0.001$), (fig. 21) but not the base or mid-cavity segments. It also correlated with, SV ($r = 0.48$, $p=0.032$), time to peak RV displacement at base and mid-cavity ($r = 0.5$, $p=0.026$), PAc ($r = 0.56$, $p=0.01$) and negatively with RVOT displacement ($r = -0.5$, $p=0.03$). In contrast, patients' time to peak RV ejection correlated mainly with the time to mid-cavity SR ($r=0.71$, $p<0.001$), (fig. 22) and to a lesser extent with the basal segment ($r=0.39$, $p=0.02$) but not with the OT. It also correlated negatively with RVOT end diastolic diameter ($r = -0.37$, $p=0.03$), PAc ($r = -0.4$, $p=0.018$) and positively with TAPSE ($r = 0.52$, $p=0.001$) and time to peak RV basal displacement ($r = 0.33$, $p=0.049$). Similar results were obtained with the non-parametric Spearman correlation analysis. In the multivariate model, time to peak systolic SR of the RVOT in controls was the strongest independent predictor of time to peak RV ejection (Beta = 0.6, $p=0.001$), as compared to PAc (Beta = -0.38, $p=0.01$). In patients, time to peak systolic SR at the mid segment (Beta = 0.65, $p=0.001$) was the only independent predictor of time to peak RV ejection.

Table 6. *LV and RV structure and function*

	Controls (n = 20)	PHT (n = 35)	p-value
Age, years	62 ± 15	67 ± 12	0.2
Heart rate, bpm	64 ± 9	75 ± 14	0.001
LVEDV, ml	96 ±14	84 ± 20	0.008
LVESV, ml	37 ± 7	35 ± 10	0.5
LA volume, ml	50 ± 8	51 ± 12	0.16
LVEF %	61 ± 2	57 ± 7	0.02
E/E' (LV)	6 ± 1	7.5 ±1.5	0.04
RV inlet diameter, cm	3 ± 0.3	4.2 ± 0.5	<0.001
RVOT EDD, cm	2.9 ± 0.3	3.7 ± 0.6	<0.001
RVOT ESD, cm	1.8 ± 0.2	3 ± 0.7	<0.001
PAc, ms^{-2}	6.6 ± 1.4	12.2 ± 6.4	0.001
TAPSE, cm	2.7 ± 0.3	1.7 ± 0.6	<0.001
PASP, mmHg	30 ± 2	67 ± 20	<0.001
MPI (RV)	0.3 ± 0.1	0.7 ± 0.2	<0.001
SV, ml	58 ± 9	49 ± 14	0.004

LV = left ventricle; RV = right ventricle; TAPSE = tricuspid annular plane systolic excursion; SV: stroke volume. PASP = pulmonary artery systolic pressure; E/E': Early LV diastolic velocity / early filling velocity from TDI; LVEF = left ventricular ejection fraction; EDV= end-diastolic volume; ESV = end systolic volume; LA = left atrium; MPI (RV) = RV myocardial performance index. RVOT = right ventricular outflow tract; EDD = end-diastolic diameter; ESD = end-systolic diameter; Pac = pulmonary ejection acceleration.

Table 7. *RV intrinsic myocardial function (STE)*

	Controls (n = 20)	PHT (n = 35)	p- value
Motion			
RV inlet velocity (STE), cm/s	9.9 ± 1.4	7.5 ± 2.4	<0.001
STE parameters			
RV (base) longitudinal strain rate, (1/s)	1.9 ± 0.5	1.3 ± 0.6	<0.001
RV (mid) longitudinal strain rate, (1/s)	1.7 ± 0.4	1 ± 0.4	<0.001
RVOT longitudinal strain rate, (1/s)	1.6 ± 0.9	1.3 ± 0.65	0.1
RV (base) longitudinal displacement (STE), mm	15.8 ± 3.6	8.5 ± 4.7	<0.001
RV (mid) longitudinal displacement (STE), mm	9 ± 3.5	4.9 ± 3.1	<0.001
RVOT longitudinal displacement (STE), mm	1.8 ± 1.1	1.7 ± 1	0.86
Timings			
Time to peak systolic strain rate at base, (ms/bpm)	3.7 ± 0.9	2.7 ± 0.9	<0.001
Time to peak systolic strain rate at mid, (ms/bpm)	3.8 ± 0.9	2.7 ± 0.9	<0.001
Time to peak systolic strain rate at RVOT, (ms/bpm)	3.8 ± 1	3 ± 1.1	0.007
Time to peak displacement at base, (ms/bpm)	6.6 ± 1.1	5 ± 1.6	<0.001
Time to peak displacement at mid, (ms/bpm)	6.6 ± 1.1	5 ± 1.6	<0.001
Time to peak displacement at RVOT, (ms/bpm)	6.6 ± 1.8	3.7 ± 1.3	<0.001

RVOT = right ventricular outflow tract; base = basal segment of right ventricle; mid = mid segment of right ventricle; STE = Speckle tracking echocardiography; RV = right ventricle

Table 8. *RV pump time relations*

	Controls(n=20)	PHT (n=35)	P-value
RV Filling time (PW), (ms/bpm)	7.4 ± 3.6	5.2 ± 2.5	0.03
Time to peak RV ejection (PW), (ms/bpm)	3.7 ± 0.7	2.8 ± 0.9	0.001
Time to end RV ejection (PW), (ms/bpm)	6.9 ± 1.2	5.6 ± 1.4	0.001
TR duration (CW), (ms/bpm)	5.7 ± 1.3	6.4 ± 1.9	0.3
Time to onset of RV filling (PW), (ms/bpm)	7.2 ± 1.5	7 ± 2	0.8
Time to onset of RV ejection (PW),(ms/bpm)	1.3 ± 0.2	1.2 ± 0.4	0.5
Time to onset of shortening (M-mode), (ms/bpm)	1.7 ± 0.3	1.4 ± 0.4	0.007
Time to peak shortening (M-mode), (ms/bpm)	6.6 ± 0.9	5.6 ± 1.8	0.009

RV = Right ventricle; PW = pulse wave spectral Doppler; TR = tricuspid regurgitation; CW = continuous wave

Intra-observer and inter-observer variability

For intra-observer reproducibility, the mean ± SD of time to peak SR at basal, mid-cavity and RVOT were: 3.7 ± 13.7 ms, 10.5 ± 14.6 ms and -1.5 ± 14.8 ms, respectively. Intraclass correlation coefficients measured by same observer were, base: 0.79 (p=0.002), mid-cavity: 0.65 (p=0.006) and RVOT: 0.87 (p<0.001). Respective values for inter-observer reproducibility were: -12.1 ± 21.3 ms, -3.8 ± 22.4 ms and -17.7 ± 23.3 ms and intraclass correlation coefficients were, base: 0.7 (p=0.005), mid: 0.69 (p=0.01) and RVOT: 0.63 (p=0.006).

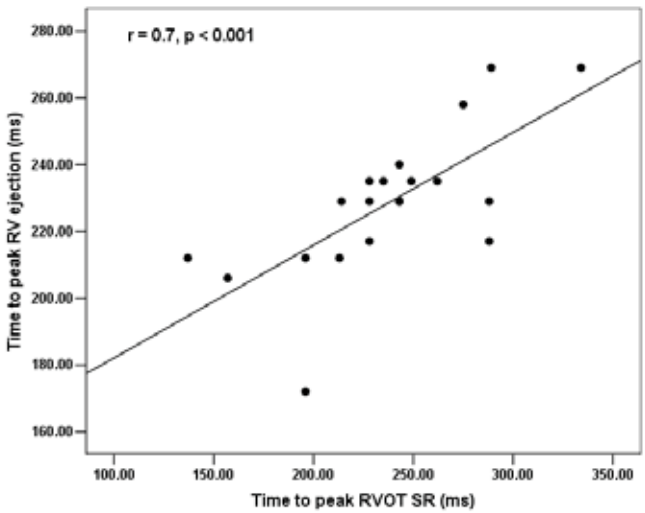

Figure 21. Segmental RVOT correlation with RV ejection in normals

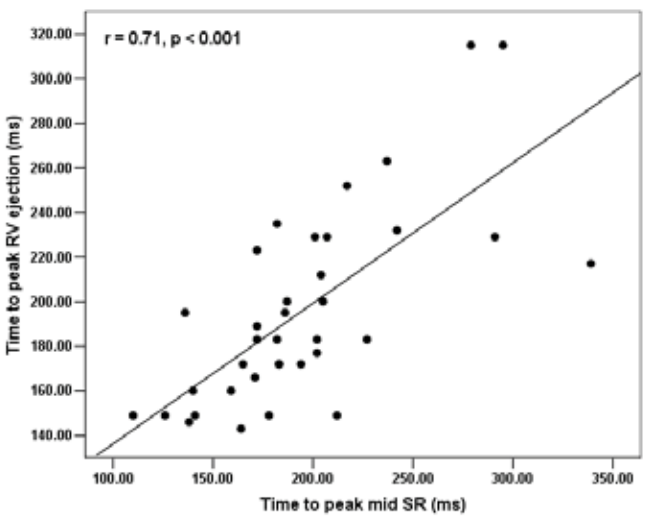

Figure 22. Segmental mid correlation with RV ejection in PH patients.

GENERAL DISCUSSION

Global review of the right ventricle

The importance of the right ventricle as a determinant of clinical symptoms, exercise capacity, peri-operative survival and post-operative outcome has been underestimated for a long time. Moreover, altered left ventricular function in patients with valvular disease influences right ventricular performance mainly by changes in afterload and also through ventricular interaction. Ejection fraction has been used as a measure of RV function but has been found to be dependent on loading conditions, ventricular interaction and myocardial structure. Right heart failure is mainly a clinical diagnosis and early detection of RV dysfunction is important and depends largely on the imaging technologies. RV function and regional wall motion can be determined with right ventricular angiography, radionuclide ventriculography, two-dimensional echocardiography or MRI with their own respective limitation. Due to the complex anatomy of the RV, assessment of its function can be problematic. The right ventricle is a crescent shaped three dimensional cavity and its transverse axis is wrapped around the LV [8]. It consists of the inflow tract, the apical 'trabecular' and the outflow tract. The inflow-outflow axis angle is significantly wider than that of the LV, an anatomical fact that requires the outflow tract to contribute significantly to the RV overall systolic function. The difference in myocardial fibre architecture of the pumps explains the difference in shape and dynamics of the two ventricles. In the light of the RV anatomy it is clear that measurement of the function of the three compartments seems to be the ideal approach. While detailed functional assessment of the outflow tract and the apical 'trabecular' compartment may be difficult to assess by echocardiography, that of the inflow tract could easily be imaged and studied by all modalities: M-Mode, Tissue-Doppler, Speckle tracking and 3D [65]. It should be remembered that although long axis function of the RV is a useful clinical measurement it does not reflect overall RV function since it does not represent the other parts of the ventricle, including the RVOT, which is the most sensitive compartment to changes in pulmonary circulation resistance and pressures [79].

In view of the above, we carried out three studies to provide more detailed assessment of RV compartmental function in terms of amplitude, timing, velocities and synchronicity. The studies,

further discussed below, have provided a clearer understanding of the functional importance of each component in health and disease.

Study 1: Differential right ventricular regional function and the effect of pulmonary hypertension: 3D echo study.

The contribution of the three RV compartments to its overall systolic function is not homogenous, with the apex the least contributor compared to the inflow and outflow tract. This pattern of function seems to be present irrespective of disease status, thus suggesting a potential additional fundamental role for the RV apex other than contraction. Its location at the relatively wide angle of crossing of the inflow and the outflow tract axes suggest a need for less power generation and minimum inward motion in order to allow efficient and smooth direction of blood towards the outflow tract. Thus, the apex has an important role in maintaining the RV intra-cavitary circulation. In addition, normally, the three RV compartments do not achieve peak volume fall simultaneously. This differential time delay is essential for maintaining the peristaltic RV pump function, in view of its shape. While this time delay remained maintained in patients with ischaemic LV disease, it was virtually lost in those who had developed additional pulmonary hypertension. This finding is of great interest because it highlights the fact that in those patients with PH the RV loses its distinct segmental function and behaves as a single chamber. The only way by which the RV can achieve this is by a significant change in its shape, becoming cylindrical rather than triangular. 3D echocardiography is unique in demonstrating such changes in pulmonary hypertension. Furthermore, this shape change was also associated with significant functional disturbances in the form of dyssynchrony during the two isovolumic times when compared to controls. With the significant reduction in the extent of volume fall during acceleration and deceleration as a reflection of intrinsic myocardial dysfunction, the RV has to use efficiently the two isovolumic phases to generate enough tension required to maintain stroke volume. This finding is further supported by the transfer of the RV outflow tract role in determining peak ejection to the apical region in patients with PH. Again this confirms the complete loss of the outflow tract integrity as it functions as part of the mono-compartmental chamber. The role of the RV inflow tract in determining peak ejection we found in the group of ischaemic LV disease patients without PH may represent a transitional stage between the normal and PH stages.

The conventional appreciation of RV inflow tract long axis motion, commonly referred to as tricuspid annulus peak systolic excursion 'TAPSE' using M-mode or tissue Doppler velocities, as the sole representative of overall RV systolic function is an underestimation and an over simplification [137] despite its close relationship to RV 3D volumes. The role of the outflow tract in determining peak ejection is a clear proof of its essential contribution to RV function [138]. Even in the absence of 3D facilities, a simple M-mode recording of RV outflow tract diameter and calculation of fractional shortening should add important information, particularly in patients with pulmonary circulation dysfunction [79]. Finally, the transfer of RV outflow tract systolic time relations to the apex in patients with PH suggests a potential benefit from electrical re-timing 'resynchronisation' of that compartment as an attempt to optimise RV stroke volume.

Study 2: Organised right ventricular remodelling in aortic stenosis even after valve replacement.

In patients with aortic stenosis, the RV is already abnormal before surgery, even in the absence of objective evidence for secondary pulmonary hypertension, the cavity is enlarged, the overall function is reduced but the outflow tract displacement is exaggerated. However, intrinsic RV myocardial function, in the form of strain rate, remains preserved. These finding may reflect a ventricular interaction phenomenon either across the interventricular septum or the intrapericardial space. In a patient with severe AS the minimum systolic LV pressure is in the order of 190 mmHg, which is significantly higher than what it is designed to manage normally [139]. In these patients increased wall tension is well known [140] and our findings suggest a transfer of that tension to the right ventricle via one or both routes mentioned above. In addition, RV inlet function seems to be compromised in contrast to the outflow tract displacement which becomes exaggerated, thus suggesting a compensatory mechanism. These changes cannot be taken lightly since they were also associated with dramatic pump function changes. The RV outflow tract loses its role in correlating with cardiac output and in determining peak ejection time, the latter function become transferred to the basal region of the RV. This particular finding is very similar to what we have previously reported, in study 1 & 3, on patients with pulmonary hypertension irrespective of its aetiology. In those patients, the raised afterload effect on RV shape makes it more cylindrical, and functionally similar to our AS patients, despite having only regional functional disturbances and less significant shape change. Furthermore, RV ejection time was significantly shorter than normal, a finding which can only be explained by some degree of dyssynchrony associating the regional dysfunction. Finally,

despite successful isolated AVR and symptomatic improvement, the RV dysfunction we found before surgery remained unchanged up to 6 months post-operatively. These findings suggest rather organic remodelling of the right ventricle before surgery which remains unchanged afterwards. They may also explain the reduced exercise capacity, after AVR, we previously reported in the same group of patients with respect to age matched controls [129]. We must also mention that the findings we reported above were not related to the pericardium which was closed post-operatively only in 50% of these patients [24].

This study adds to the body of knowledge that RV function is of great importance in patients with left ventricular pathology, irrespective of its aetiology. Although our patients had what is clinically described as isolated aortic stenosis i.e. with normal LV ejection fraction and no coronary artery disease, RV function was before and remained after AVR significantly impaired. Thus, in severe AS delaying valve replacement might only result in further deterioration of right and left ventricular function, which might become irreversible and hence devaluing a successful operation**.**

Study 3: Global and regional right ventricular disturbances in patients with pulmonary hypertension and normal left ventricular function.

Raised RV afterload in the form of PH has significant effect on its function involving its three compartments in 4 different dimensions: amplitude of motion, velocities, myocardial strain rate and its time relations. The cavity was dilated with significantly reduced function, particularly at the basal level, a region commonly used to reflect overall RV performance i.e. ejection fraction [141]. This was not only in the form of reduced TAPSE but also compromised intrinsic myocardial function as shown by SR measurements, including its early peaking. Interestingly, the early SR timing was what determined RV peak ejection time, although in completely two different ways between controls and patients. While in normal RVOT regional function determined its peak ejection time, in PH patients this function was transferred to the mid RV cavity. This suggests that RVOT does not only use its contractile function but also its gate keeping properties, being the closest to the raised pulmonary resistance. The transfer of that regional function to the mid RV segments suggests an evidence for RV remodeling in PH. It must be emphasised that SR measurements were unique in showing significant differences between patients and controls, confirming their sensitivity to even early changes in PH.

Our findings reproduce what we previously reported, in study 1, on the changes in RV structure and function in a different group of patients with PH, secondary to ischemic LV dysfunction and raised LA pressure, in whom RVOT relationship with peak ejection was similarly transferred to mid-cavity compartment [142], despite using a different echocardiographic technique, i.e. 3D technology. Thus, it seems that irrespective of the etiology of PH, RV response and functional changes are almost similar. Finally, the short RV filling time, in the absence of delayed filling is consistent with additional cavity dyssynchrony as a result of either the delayed conduction speed, commonly seen in PH patients (50% of our patients had QRS duration >100 ms) or primary myocardial dysfunction. This suggestion is supported by the significantly raised RV myocardial performance index in patients with respect to controls similar to what we and others have previously shown in the left heart [143].

The impairment of RV function following long standing PH is not only structural but more importantly functional with significant fall in intrinsic myocardial function and disturbed time relations, consistent with significant shape change of the RV from three compartmental pump into a more cylindrical one with different geometric properties. In view of our findings it appears that in PH the RV loses its peristaltic function and its propelling function becomes controlled by the mid cavity region. As an attempt to normalise RV time relations we propose that pacing RVOT and optimising its time delay with respect to mid-cavity might improve its ejection function and potentially patients' clinical condition. Finally, the unique alteration of SR timing of the RVOT suggests its clinical relevance as a potential early predictor of RV dysfunction in PH, before the commonly used TAPSE. This finding might be of help in identifying patients needing more aggressive PH treatment in order to stop or delay RV progression into irreversible shape change and cavity remodelling.

Limitations of studies

In study 1, the patient sample volume we studied was small. We did not study patients with primary idiopathic PAH since our study plan was to document normal RV function and the effect of the commonest cause of RV dysfunction in clinical practice rather than individual relatively rare conditions. We intentionally elected to document the most clinically applicable findings which are likely to assist clinicians and echocardiographers to appreciate the extent of complexity of RV function as well as the nature and severity of disturbances seen in PH. We were unable to exclude the potential role of ventricular interaction, in PH, in affecting our

results and the differences between groups. Finally, the strikingly low normal SV calculated from RV volumes, as previously shown [144], with respect to PH patients highlights the technical limitation of the 3D in assessing SV. This could be explained by the complex inlet anatomy which results in limited endocardial delineation and suboptimal volume assessment. This limitation is partially overcome in PH patients, in whom the RV inlet compartment is dilated and the endocardium better delineated and hence more accurate volume estimation. We are confident that we applied the landmarks of the three RV compartments previously recommended by cardiac morphologists [117].

Our study 2 had some limitations. We did not have invasive pressure measurements of the right heart, which might have helped in data interpretation but excluded the presence of secondary pulmonary hypertension based on the normal right atrial size and the normal retrograde pressure drop across the tricuspid valve**.** We did not study radial strain rate of the RVOT but only the longitudinal SR to ease comparison with the inflow part. We did not use RV volumes to calculate SV due to its complex geometry, but only relied on the LVOT diameter and VTI measurements. Our suggestion of ventricular interaction via the septum or intra-pericardial space is based on our knowledge of normal cardiac physiology particularly in aortic stenosis. Our cohort is small, however findings were consistent.

In study 3, we did not use 3- dimensional echocardiography to assess the nature of changes in RV geometry, which would have assisted in explaining the findings, but relied on our previously reported interpretation of similar findings in secondary PH, in the first study. We suggested that the short RV filling is a sign of cavity dyssynchrony but do not have additional means for confirming this explanation, since there is no standardized means for assessing RV dyssynchrony in such patients. We did not study radial strain rate of the RVOT but only the longitudinal SR to ease comparison with the inflow part. We did not have the arterial blood pressure on the patients that could account in post-capillary PH due to raised LA pressure. Our selection criteria were a small cohort of PH patients with mixed aetiologies. However, the present study did not allow for evaluation of the impact of a specific PH disease on the accuracy of echocardiographic indices.

CONCLUSIONS

1. Normal right ventricular shape and function are asymmetrical with clearly defined three compartments of different systolic capacity and time relations. This distinct pattern is virtually lost in patients with pulmonary hypertension, who exhibit clear evidence for gross dyssynchrony during the two isovolumic periods. For those with deteriorating RV decompensation despite optimal medical treatment, electrical re-timing of RV outflow tract might optimise pump efficiency and control symptoms.

2. The right ventricle is significantly abnormal in structure and function in compensated aortic stenosis. The cavity is dilated and regional and segmental function are quite impaired and remain unchanged at mid-term after AVR. These findings suggest an organised remodelling process secondary to ventricular interaction, which may also explain these patients' reduced exercise capacity. Thus, delaying valve replacement for aortic stenosis might result in irreversible damage of the ventricles and less satisfactory surgical results.

3. Pulmonary hypertension has drastic effects on RV structure and intrinsic myocardial function, significantly disturbing its ejection time relations and overall pump performance. Early identification of such changes might help in identifying patients who need more aggressive therapy early on in the disease process.

ACKNOWLEDGMENTS

This research project would not have been possible without the help and support of a number of individuals as well as the collaboration of various institutions and their respective departments.

Firstly, I would like to express my deepest gratitude to my supervisor, Michael Y Henein, for his endless help and support throughout my PhD research. He is the first person who introduced me to the real research world. My research path has been much easier and rewarding thanks to his patience, encouragement, motivation, quick response and through sharing his great knowledge. Thanks for always being available, despite being in another part of the world from time to time.

Secondly, I would like to thank Per Lindqvist, my co-supervisor for sharing his great knowledge on the subject of my thesis. His constructive criticism and support has helped me to make this book possible. Also, I wish to thank him for introducing me to the EchoPac software as well as performing most of the echoes on the patients included in my second and third paper.

I would also wish to thank Stefan Soderberg, co-author, who performed all the cardiac catheterisation on the patients included in my third paper as well as for the constructive criticism and help in producing one of the manuscripts.

Thank you to Anders Holmgren, co-author, who performed surgery on all the patients included in the second paper.

Special thanks to:-

- Sandra Gustaffson from the Echo department for performing some of the echoes on patients included in my second paper.

- Ying Zhao for sharing her knowledge in the field of statistics.

- Kerstin Rosenqvist for her extensive administrative support, Swedish translation and email correspondence. I will always remember her warm welcome during my research visits to the department.

- Eva Jonasson for her warm welcome during my time in Umeå and for taking care of my hotel bookings during my various stays.

I also wish to thank Marilyn Stanton and Valerie Cyster as well as all the staff and friends of West Middlesex University Hospital UK, for their continuous support and help.

My sincere respect and thanks to Prof Margaret Hodson, co-author, of Royal Brompton Hospital UK for accommodating me in her department, to analyse the data for my first paper.

A special thanks goes to Robin Chung, co-author, for his help and support, as well as his great knowledge in producing my first paper.

Finally but most importantly, I am grateful to my mum and dad, my brother and sister in law, cousins and Sweety, my fiancée, for their love, help, support and encouragement.

REFERENCES

1. Baker BJ, Wilen MM, Boyd CM, Dinh H, Francisa JA. Relation of right ventricular ejection fraction to exercise capacity of patients with chronic left ventricular failure. Am J Cardiol 1984;54:596-9.

2. Enger R, Ray R, Higgins CB. Clinical assessment and follow up of functional capacity in patients with chronic congestive cardiomyopathy. Am J Cardiol 1982;49:1832-7.

3. Ho SY, Nihoyannopoulos P. Anatomy, echocardiography and normal right ventricular dimensions. Heart 2006;92(suppl.l):i2-i3.

4. Bleeker GB, Steendijk P, Holman ER, Yu CM, Breithardt OA, Kaandorp TAM, Schalij MJ, Van der Wall EE, Bax JJ, Nihoyannopoulos P. Acquired right ventricular dysfunction. Heart 2006;92:14-18.

5. Dell'Italia LJ, Santamore WP. Can indices of the left ventricular function be applied to the right ventricle?. Prog Cardiovasc Dis. 1998;40:309-24.

6. Foale R, Nihoyannopoulos P, McKenna W, Kleinebenne A, Nadazdin A, Rowland E, et al. Echocardiographic measurement of the normal adult right ventricle. Br Heart J 1986;56:33–44.

7. Goor DA, Lillehei CW. Congenital malformations of the heart, 1st ed. New York: Grune and Stratton, 1975:1–37.

8. Dell'Italia LJ. The right ventricle: anatomy, physiology, and clinical importance. Curr Probl Cardiol 1991;16:653–720.

9. Grant RP, Downey FM, MacMahon H. The architecture of the right ventricular outflow tract in the normal human heart and in the presence of ventricular septal defects. Circulation 1961;24:223–35.

10. Henein MY, Zhao Y, Nicholl R, Sun L, Khir AW, Franklin K, et al. The human heart: application of the golden ratio and angle. Int J Cardiol 2011;150:239-42.

11. Greenbaum RA, Ho SY, Gibson DG, Becker AE, Anderson RH. Left ventricular fibre architecture in man. Br Heart J 1981;45:248-63.

12. Torrent-Guasp F. Structure and function of the heart. Rev Esp Cardiol 1998;51:91-102.

13. Grant R DFaMH. The Architecture of the right ventricular outflow tract in the normal human heart and in the presence of ventricular septal defects. Circulation 1961;XXIV:223-235.

14. Armour JA, Randall WC. Structural basis of cardiac function. Am J Physiol 1970;218:1517-23.

15. Gibson D. The Right Ventricular Infundibulum: Has it a role? Eur J Echocardiogr 2003;4:3.

16. Keith A. Fate of the bulbus cordis in the human heart. Lancet 1924:1267-1273.

17. Izumo M, Shiota M, Saitoh T, Kuwahara E, Fukuoka Y, Gurudevan SV, et al. Non-circular shape of right ventricular outflow tract: a real-time 3-dimensional transesophageal echocardiography study. Circ Cardiovasc Imaging 2012;5:621-7.

18. Rushmer RF TW. The mechanism of ventricular contraction: A cinefluorographic study. Circulation 1951;4:219-228.

19. Torrent-Guasp F, Buckberg GD, Clemente C, Cox JL, Coghlan HC, Gharib M. The structure and function of the helical heart and its buttress wrapping. I. The normal macroscopic structure of the heart. Semin Thorac Cardiovasc Surg 2001;13:301-19.

20. Buckberg GD, Coghlan HC, Hoffman JI, Torrent-Guasp F. The structure and function of the helical heart and its buttress wrapping. VII. Critical importance of septum for right ventricular function. Semin Thorac Cardiovasc Surg 2001;13:402-16.

21. Geva T, Powell AJ, Crawford EC, Chung T, Colan SD. Evaluation of regional differences in right ventricular systolic function by acoustic quantification echocardiography and cine magnetic resonance imaging. Circulation 1998;98:339-345.

22. Kaul S. The interventricular septum in health and disease. Am Heart J 1986;112:568-81.

23. Klima U, Guerrero JL, Vlahakes GJ. Contribution of the interventricular septum to maximal right ventricular function. Eur J Cardiothorac Surg 1998;14:250-5.

24. Lindqvist P, Holmgren A, Zhao Y, Henein MY. Effect of pericardial repair after aortic valve replacement on septal and right ventricular function. Int J Cardiol 2012;155:388-93.

25. Gaynor SL, Maniar HS, Prasad SM, Steendijk P, Moon MR. Reservoir and conduit function of right atrium: impact on right ventricular filling and cardiac output. Am J Physiol Heart Circ Physiol 2005;288:H2140-5.

26. Fujii J, Yazaki Y, Sawada H, Aizawa T,Watanabe H, Kato K. Noninvasive assessment of left and right ventricular filling in myocardial infarction with a two-dimensional Doppler echocardiographic method. J Am Coll Cardiol 1985;5:1155-60.

27. Yanase O, Motomiya T, Tejima T, Nomura S. Doppler echocardiographic assessment of right ventricular filling characteristics in hemodynamically significant right ventricular infarction. Am J Noninvasiv Cardiol 1992;6:230-6.

28. Yilmaz M, Erol MK, Acikel M, Sevimli S, Alp N. Pulsed Doppler tissue imaging can help to identify patients with right ventricular infarction. Heart Vessels 2003;18:112-6.

29. Rudski LG, Lai WW, Afilalo J, Hua L, Handschumacher MD, Chandrasekaran K, et al. Guidelines for the Echocardiographic Assessment of the Right Heart in Adults: A Report from the American Society of Echocardiography, endorsed by the European Association of Echocardiography, a registered branch of the European Society of Cardiology, and the Canadian Society of Echocardiography. J Am Soc Echocardiogr 2010;23:685-713.

30. Grose R, Strain J, Yipintosoi T. Right ventricular function in valvular heart disease: relation to pulmonary artery pressure. J Am Coll Cardiol 1983;2:225-32.

31. Morrison DA, Goldman S, Wright AL, et al. The effect of pulmonary hypertension on systolic function of the right ventricle. Chest 1983;84:250-7.

32. Nienaber CA, Spielmann RP, Wasmus G, Montz R, Mathey DG, Bleifeld DG. Right ventricular ejection fraction from equilibrium krypton-81 m blood pool scans: a noninvasive predictor of pulmonary artery hypertension. Eur Heart J 1987;8:297-307.

33. Hirata N, Sakakibara T, Shimazaki Y, et al. Preoperative and postoperative right ventricular function during exercise in patients with mitral stenosis. J Thorac Cardiovasc Surg 1992;104:1029-34.

34. Nagel E, Stuber M, Hess OM. Importance of the right ventricle in valvular heart disease. Eur Heart J 1996;17:829-836. Review.

35. Unterberg R, Rommich P, Volker W, Mauser M, Karsch KR. EinfluB der Volumenbelastung des linken Ventrikels bei Aorten- und Mitralinsuffizienz auf die Geometrie und Funktion der rechten Kammer. Z Kardiol 1987;76:761-9.

36. Villari B, Hess OM, Meier C, et al. Regression of coronary artery dimensions after successful aortic valve replacement. Circulation 1992;85:972-8.

37. Vassalli G, Hess OM, Krogmann ON, et al. Coronary artery size in mitral regurgitation and its regression after mitral valve surgery Am Heart J 1993;126:1091-8.

38. Brilla C, Konz KH, Karsch KR, Seipel L. Right ventricular function in mitraVaortic valve disease with and without tricuspid incompetence. Z Kardiol 1986; 75 (Suppl 2): 114-6.

39. Unterberg R, Konig S, Volker W, Piesch-Breifeld B, Karsch KR. Funktion des rechten Ventrikels bei Patinten mit Mitralvitien. Z Kardiol 1989; 78: 386-93.

40. Jurcut R, Giusca S, Ticulescu R, Popa E, Amzulescu MS, Ghiorghiu I, et al. Different patterns of adaptation of the right ventricle to pressure overload: a comparison between pulmonary hypertension and pulmonary stenosis. J Am Soc Echocardiogr 2011;24:1109-17.

41. Henein MY. Ventricular long axis function. [Thesis]. 1997.

42. Burgess MI, Bright-Thomas RJ, Ray SG. Echocardiograghic evaluation of right ventricular function. Eur J Echocardiogr 2002;3:252-62.

43. Yoshifuku S, Otsuji Y, Takasaki K, Yuge K, Kisanuki A, Toyonaga K, et al. Pseudonormalized Doppler total ejection isovolume (Tei) index in patients with right ventricular acute myocardial infarction. Am J Cardiol 2003;91:527-31.

44. Ribeiro A, Lindmarker P, Juhlin-Dannfelt A, Johnsson H, Jorfeldt L. Echocardiography Doppler in pulmonary embolism: right ventricular dysfunction as a predictor of mortality rate. Am heart J 1997;134:479-87.

45. Morrison DA, Ovitt T, Hammermeister KE. Functional tricuspid regurgitation and right ventricular dysfunction in pulmonary hypertension. Am J Cardiol 1988;62:108-12.

46. Morrison DA, Lancaster L, Henry R, Goldman S, Turgeon J. Right ventricular function at rest and during exercise in aortic and mitral valve disease. J Am Coll Cardiol 1985;5:21-8.

47. Braunwald NS, Ross J Jr, Morrow AG. Conservative management of tricuspid regurgitation in patients undergoing mitral valve replacement. Circulation 1967;35:163-9.

48. Simon R, Oelert H, Borst HG, Lichtlen PR. Influence of mitral valve surgery on tricuspid incompetence concomitant with mitral valve disease. Circulation 1980;62:1152-7.

49. Duran CMG, Pomar JL, Colman T, Figueroa A, Revuelta JM, Ubago JL. Is tricuspid valve repair necessary? J Thorac Cardiovasc Surg 1980;80:849-60.

50. Breyer RH, McClenathan JH, Michaelis LL, Mclntosch CL, Morrow AG. Tricuspid regurgitation. A comparison of nonoperative management, tricuspid annuloplasty and tricuspid valve replacement. J Thorac Cardiovasc Surg 1976;72:867-74.

51. Wranne B, Pinto FJ, Hammarstrom E, St Goar FG, Puryear J, Popp RL. Abnormal right heart filling after cardiac surgery: time course and mechanisms. Br Heart J 1991;66:435-42.

52. Carr-White GS, Kon M, Koh TW, Glennan S, Ferdinand FD, De Souza AC, et al. Right ventricular function after pulmonary autograft replacement of the aortic valve. Circulation 1999;100(19 Suppl):II36-41.

53. Henein MY, O'Sullivan CA, Coats AJ, Gibson DG. Angiotensin-converting enzyme (ACE) inhibitors revert abnormal right ventricular filling in patients with restrictive left ventricular disease. J Am Coll Cardiol 1998;32:1187–93.

54. Ribeiro A, Lindmarker P, Johnsson H, Juhlin-Dannfelt A, Jorfeldt L. Pulmonary embolism: a follow-up study of the relation between the degree of right ventricle overload and the extent of perfusion defects. J Intern Med 1999;245:601-10.

55. Gomez A, Bialostozky D, Zajarias A, Santos E, Palomar A, Martinez ML, et al. Right ventricular ischaemia in patients with primary pulmonary hypertension. J Am Coll Cardiol 2001;38:1137-42.

56. O'Sullivan CA, Duncan A, Daly C, Li W, Oldershaw P, Henein MY. Dobutamine stress-induced ischemic right ventricular dysfunction and its relation to cardiac output in patients with three-vessel coronary artery disease with angina-like symptoms. Am J Cardiol 2005;96:622-7.

57. Goldstein JA. Right heart ischaemia: pathophysiology, natural history, and clinical management. Prog Cardiovasc Dis 1998;40:325-41.

58. Matthay RA, Berger HJ. Non-invasive assessment of right and left ventricular function in acute and chronic respiratory failure. Crit Care Med 1983;11:329-38.

59. Brent BN, Mahler D, Berger HJ, Matthay RA, Pytlik L, Zaret BL. Augmentation of right ventricular performance in chronic obstructive pulmonary disease by terbutaline: a combined radionuclide and hemodynamic study. Am J Cardiol 1982;50:313-9.

60. Brent BN, Berger HJ, Matthay RA, Mahler D, Pytlik L, Zaret BL. Physiologic correlates of right ventricular ejection fraction in chronic obstructive pulmonary disease: a combined radionuclide and hemodynamic study. Am J cardiol 1982;50:255-62.

61. Mahler DA, Brent BN, Loke J, Zaret BL, Matthay RA. Right ventricular performance and central circulatory hemodynamics during upright exercise in patients with chronic obstructive pulmonary disease. Am Rev Respir Dis 1984;130:722-9.

62. Florea VG, Florea ND, Sharma R, Coats AJ, Gibson DG, Hodson ME, et al. Right ventricular dysfunction in adult severe cystic fibrosis. Chest 2000;118:1063-8.

63. Nakamura K, Miyahara Y, Ikeda S, Naito T. Assessment of right ventricular diastolic function by pulsed Doppler echocardiography in chronic pulmonary disease and pulmonary thromboembolism. Respiration 1995;62:237-43.

64. Hoffman D, Sisto D, Frater RWM, Nikolic SD. Left-to-right ventricular interaction with a noncontracting right ventricle. J Thorac Cardiovasc Surg 1994;107:1496-502.

65. Lindqvist P, Calcutteea A, Henein MY. Echocardiography in the assessment of right heart function. Eur J Echocardiogr 2008;9:225-234.

66. Henein MY, Gibson DG. Suppression of left ventricular early diastolic filling by long axis asynchrony. Br Heart J 1995;73:151-7.

67. Slinker BK, Glantz SA. End-systolic and end-diastolic ventricular interaction. Am J Physiol 1986;251:H1062-75.

68. Hess OM, Bhargava V, Ross J Jr, Shabetai R. The role of the pericardium in interactions between the cardiac chambers. Am Heart J 1983;106:1377-83.

69. Henein M, Sheppard M, Pepper J, Rigby M. Clinical echocardiography. London: Springer; pp.195–209.

70. Beygui F, Furber A, Delepine S, Helft G, Metzger JP, Geslin P, et al. Routine breath-hold gradient echo MRI-derived right ventricular mass, volumes and function: accuracy, reproducibility and coherence study. Int J Cardiovasc Imaging 2004;20:509-16.

71. Pini R, Giannazzo G, Di BM, Innocenti F, Rega L, Casolo G, et al. Transthoracic three-dimensional echocardiographic reconstruction of left and right ventricles: in vitro validation and comparison with magnetic resonance imaging. Am Heart J 1997;133:221-9.

72. Marving J, Hoilund-Carlsen PF, Chraemmer-Jorgensen B, Gadsbell N. Are right and left ventricular ejection fractions equal? ejection fractions in normal subjects and in patients with first acute myocardial infarction. Circulation 1985;72:502-14.

73. Dell'Italia LJ, Starling MR, Walsh RA, Badke FR, Lasher JC, Blumhardt R. Validation of attenuation-corrected equilibrium radionuclide angiogaphic determinations of right ventricular volume: comparison with cast-validated biplane cineventriculography. Circulation 1985;72:317-26.

74. Manno BV, Iskandrian AS, Hakki AH. Right ventricular function: methodologic and clinical condiderations in noninvasive scintigraphic assessment. J Am Coll Cardiol 1984;3:1072-81.

75. Nichols K, Saouaf R, Ababneh AA, Barst RJ, Rosenbaum MS, Groch MW, et al. Validation of SPECT equilibrium radionuclide angiographic right ventricular parameters by cardiac magnetic resonance imaging. J Nucl Cardiol 2002;9:153-60.

76. Hoffmann R, Hanrath P. Tricuspid annular velocity measurement. Simple and accurate solution for a delicate problem? Eur Heart J 2001;22:280–2.

77. Kaul S, Tei C, Hopkins JM, Shah PM. Assessment of right ventricular function using two-dimensional echocardiography. Am Heart J 1984;107:526–31.

78. Ghio S, Gavazzi A, Campana C, Inserra C, Klersy C, Sebastiani R et al. Independent and additive prognostic value of right ventricular systolic function and pulmonary artery pressure in patients with chronic heart failure. J Am Coll Cardiol 2001;37:183–8.

79. Lindqvist P, Henein M, Kazzam E. Right ventricular outflow tract fractional shortening: an applicable measure of right ventricular systolic function. Eur J Echocardiogr 2003;4:29–35.

80. Forni G, Pozzoli M, Cannizzaro G, Traversi E, Calsamiglia G, Rossi D et al. Assessment of right ventricular function in patients with congestive heart failure by echocardiographic automated boundary detection. Am J Cardiol 1996;78:1317–21.

81. Vignon P, Weinert L, Mor-Avi V, Spencer KT, Bednarz J, Lang RM. Quantitative assessment of regional right ventricular function with color kinesis. Am J Respir Crit Care Med 1999;159:1949–59.

82. Currie PJ, Seward JB, Chan KL, Fyfe DA, Hagler DJ, Mair DD, et al. Continuous wave Doppler determination of right ventricular pressure: a simultaneous Doppler-catheterization study in 127 patients. J Am Coll Cardiol 1985;6:750-6.

83. Daniels LB, Krummen DE, Blanchard DG. Echocardiography in pulmonary vascular disease. Cardiol Clin 2004;22:383-99.

84. Tei C, Dujardin KS, Hodge DO, Bailey KR, McGoon MD, Tajik AJ, et al. Doppler echoardiographic index for assessment of global right ventricular function. J Am Soc Echocardiogr 1996;9:838-47.

85. Eidem BW, Tei C, O'Leary PW, Cetta F, Seward JB. Nongeometric quantitative assessment of right and left ventricular function: myocardial performance index in normal children and patients with Ebstein anomaly. J Am Soc Echocardiogr 1998;11:849–56.

86. Eidem BW, O'Leary PW, Tei C, Seward JB. Usefulness of the myocardial performance index for assessing right ventricular function in congenital heart disease. Am J Cardiol 2000;86:654–8.

87. Hatle L, Sutherland GR. Regional myocardial function—a new approach. Eur Heart J 2000;21:1337- 5.

88. Isaaz K, Munoz del Romeral L, Lee E, Schiller NB. Quantitation of the motion of the cardiac base in normal subjects by Doppler echocardiography. J Am Soc Echocardiogr 1993;6:166–76.

89. Yalcin F, Kaftan A, Muderrisoglu H, Korkmaz ME, Flachskampf F, Garcia M et al. Is Doppler tissue velocity during early left ventricular filling preload independent? Heart 2002;87:336–9.

90. Marwick TH. Clinical applications of tissue Doppler imaging: a promise fulfilled. Heart 2003;89:1377–8.

91. Lind B, Nowak J, Dorph J, van der Linden J, Brodin LA. Analysis of temporal requirements for myocardial tissue velocity imaging. Eur J Echocardiogr 2002;3:214–9.

92. Padeletti M, Cameli M, Lisi M, Zacà V, Tsioulpas C, Bernazzali S, Maccherini M, Mondillo S. Right atrial speckle tracking analysis as a novel noninvasive method for pulmonary hemodynamics assessment in patients with chronic systolic heart failure. Echocardiography 2011;28:658-64.

93. Badano LP, Ginghina C, Easaw J, Muraru D, Grillo MT, Lancellotti P, Pinamonti B, Coghlan G, Marra MP, Popescu BA, De Vita S. Right ventricle in pulmonary arterial hypertension: haemodynamics, structural changes, imaging, and proposal of a study protocol aimed to assess re-modelling and treatment effects. Eur J Echocardiogr 2010;11:27-37.

94. Papavassiliou DP, Parks WJ, Hopkins KL, Fyfe DA. Three dimensional echocardiographic measurement of right ventricular volume in children with congenital heart disease validated by magnetic resonance imaging. J Am Soc Echocardiogr 1998;11:770–7.

95. Jiang L, Siu SC, Handschumacher MD, Luis Guererro J, Vazquez de Prada JA, King ME, et al. Three-dimensional echocardiography. In vivo validation for right ventricular volume and function. Circulation 1994;89:2342–50.

96. Kjaergaard J, Sogaard P, Hassager C. Quantitative echocardiographic analysis of the right ventricle in healthy individuals. J Am Soc Echocardiogr 2006;19:1365–72.

97. Galie N, Torbicki A, Barst R et al. Guidelines and diagnosis and treatment of pulmonary arterial hypertension. Rev Esp Cardiol 2005;58:523-66.

98. Galie N, Hoeper MM, Humbert M, Torbicki A, Vachiery JL, Barbera JA,et al. Guidelines for the diagnosis and treatment of pulmonary hypertension: the Task Force for the Diagnosis and Treatment of Pulmonary Hypertension of the European Society of Cardiology (ESC) and the European Respiratory Society (ERS), endorsed by the International Society of Heart and Lung Transplantation (ISHLT). Eur Heart J 2009;30:2493-537.

99. Celermajer DS, Marwick T. Echocardiographic and right heart catheterization techniques in patients with pulmonary arterial hypertension. Int J Cardiol 2008;125:294-303.

100. Chemla D, Castelain V, Humbert M, Hébert JL, Simonneau G, Lecarpentier Y, et al. New formula for predicting mean pulmonary artery pressure using systolic pulmonary artery pressure. Chest 2004;126:1313-1317.

101. López-Candales A, Dohi K, Rajagopalan N, Edelman K, Gulyasy B, Bazaz R. Defining normal variables of right ventricular size and function in pulmonary hypertension: an echocardiographic study. Postgrad Med J 2008;84:40-5.

102. Zoghbi WA, Enriquez-Sarano M, Foster E, Grayburn PA, Kraft CD, Levine RA, Nihoyannopoulos P, Otto CM, Quinones MA, Rakowski H, Stewart WJ, Waggoner A, Weissman NJ. Recommendations for evaluation of the severity of native valvular regurgitation with two-dimensional and Doppler echocardiography. J Am Soc Echocardiogr 2003;16:777-802.

103. Dabestani A, Mahan G, Gardin JM, Takenaka K, Burn C, Allfie A et al. Evaluation of pulmonary artery pressure and resistance by pulsed Doppler echocardiography. Am J Cardiol 1987;59:662–8.

104. Hatle L, Angelsen BA, Tromsdal A. Non-invasive estimation of pulmonary artery systolic pressure with Doppler ultrasound. Br Heart J 1981;45:157–65.

105. Kitabatake A, Inoue M, Asao M, Masuyama T, Tanouchi J, Morita T, et al. Noninvasive evaluation of pulmonary hypertension by a pulsed Doppler technique. Circulation 1983;68:302-9.

106. Stein PD, Sabbah HN, Anbe DT, Marzilli M. Performance of the failing and nonfailing right ventricle of patients with pulmonary hypertension. Am J Cardiol 1979;44:1050-5.

107. Zimbarra Cabrita I, Ruisanchez C, Grapsa J, Dawson D, North B, Pinto FJ, et al. Validation of the isovolumetric relaxation time for the estimation of pulmonary systolic arterial blood pressure in chronic pulmonary hypertension. Eur Heart J Cardiovasc Imaging 2013;14:51-5.

108. Bréchot N, Gambotti L, Lafitte S, Roudaut R. Usefulness of right ventricular isovolumic relaxation time in predicting systolic pulmonary artery pressure. Eur J Echocardiogr 2008;9:547.

109. Lindqvist P, Henein MY. Right ventricular function in pulmonary hypertension. Imaging Med 2012;4:657–665.

110. Abbas AE, Fortuin FD, Schiller NB, Appleton CP, Moreno CA, Lester SJ. A simple method for noninvasive estimation of pulmonary vascular resistance. J Am Coll Cardiol 2003;41:1021-7.

111. Lindqvist P, Soderberg S, Gonzalez MC, Tossavainen E, Henein MY. Echocardiography based estimation of pulmonary vascular resistance in patients with pulmonary hypertension: a simultaneous Doppler echocardiography and cardiac catheterization study. Eur J Echocardiogr 2011;12:961-6.

112. Quinones MA, Otto CM, Stoddard M, Waggoner A, Zoghbi WA. Recommendations for quantification of Doppler echocardiography: a report from the Doppler Quantification Task Force of the Nomenclature and Standards Committee of the American Society of Echocardiography. J Am Soc Echocardiogr 2002;15:167-84.

113. Rajagopalan N, Simon MA, Shah H, Mathier MA, Lopez-Candales A. Utility of right ventricular tissue Doppler imaging: correlation with right heart catheterization. Echocardiography 2008;25:706-11.

114. Lopez-Candales A, Dohi K, Rajagopalan N, Suffoletto M, Murali S, Gorcsan J, et al. Right ventricular dyssynchrony in patients with pulmonary hypertension is associated with disease severity and functional class. Cardiovasc Ultrasound 2005;3:23.

115. Fukuda Y, Tanaka H, Sugiyama D, Ryo K, Onishi T, Fukuya H, et al. Utility of right ventricular free wall speckle-tracking strain for evaluation of right ventricular performance in patients with pulmonary hypertension. J Am Soc Echocardiogr. 2011 Oct;24:1101-8.

116. Kasner M, Westermann D, Steendijk P, Drose S, Poller W, Schultheiss HP, et al. LV Dysfunction Induced by a Non-severe Idiopathic Pulmonary Arterial Hypertension. A Pressure-Volume Relationship Study. Am J Respir Crit Care Med 2012;186:181- 3.

117. Anderson RH, Ho SY. What is a ventricle?. Ann Thoracic Surg 1998;66:616-20.

118. Anderson RH, Razavi R, Taylor AM. Cardiac anatomy revisited. J Anat 2004;205:159 - 77.

119. Bodhey NK, Beerbaum P, Sarikouch S, et al. Functional analysis of the components of the right ventricle in the setting of tetralogy of Fallot. Circ Cardiovasc Imaging 2008;1:141–7.

120. Horton KD, Meece RW, Hill JC. Assessment of the right ventricle by echocardiography: a primer for cardiac sonographers. J Am Soc Echocardiogr 2009;22:776-792.

121. Sharma UC, Barenbrug P, Pokharel S, Dassen WR, Pinto YM, Maessen JG. Systematic review of the outcome of aortic valve replacement in patients with aortic stenosis. Ann Thorac Surg 2004;78: 90–5.

122. Iwahashi N, Nakatani S, Kanzaki H, Hasegawa T, Abe H, Kitakaze M. Acute improvement in myocardial function assessed by myocardial strain and strain rate after aortic valve replacement for aortic stenosis. J Am Soc Echocardiogr 2006;19:1238–44.

123. Lindqvist P, Bajraktari G, Molle R, Palmerini E, Holmgren A, Mondillo S, et al. Valve replacement for aortic stenosis normalizes subendocardial function in patients with normal ejection fraction. Eur J Echocardiogr 2010;11:608–13.

124. Maslow AD, Regan MM, Schwartz C, Bert A, Singh A. Inotropes improve right heart function in patients undergoing aortic valve replacement for aortic stenosis. Anesth Analg 2004; 98:891-902.

125. Roshanali F, Yousefnia MA, Mandegar MH, Rayatzadeh H, Alinejad S. Decreased right ventricular function after coronary artery bypass grafting. Tex Heart Inst J 2008;35:250-5.

126. Sun JP, James KB, Yang XS, Solankhi N, Shah MS, Arheart KL, et al. Comparison of mortality rates and progression of left ventricular dysfunction in patients with idiopathic dilated cardiomyopathy and dilated versus non-dilated right ventricular cavities. Am J Cardiol 1997;80:1583-7.

127. Patel AR, Dubrey SW, Mendes LA, Skinner M, Cupples A, Falk RH, et al. Right ventricular dilatation in primary amyloidosis: an independent predictor of survival. Am J Cardiol 1997; 80:486-92.

128. De Groote P, Millaire A, Foucher-Hossein C, Nugue O, Marchandise X, Ducloux G, et al. Right ventricular ejection fraction is an independent predictor of survival in patients with moderate heart failure. J Am Coll Cardiol 1998;32:948-54.

129. Zhao Y, Henein MY, Morner S, Gustavsson S, Holmgren A, Linqvist P. Residual compromised myocardial contractile reserve after valve replacement for aortic stenosis. Eur Heart J Cardiovasc Imaging 2012;13:353-60.

130. Sato T, Tsujino I, Ohira H, Oyama-Manabe N, Yamada A, Ito YM, et al. Validation study on the accuracy of echocardiographic measurements of right ventricular systolic function in pulmonary hypertension. J Am Soc Echocardiogr 2012;25:280-6.

131. Birks EJ, Yacoub MH, Anyanwu A, Smith RR, Banner NR, Khaghani A. Transplantation using hearts from primary pulmonary hypertensive donors for recipients with a high pulmonary vascular resistance. J Heart Lung Transplant 2004;23:1339-44.

132. Steiropoulos P, Trakada G, Bouros D. Current pharmacological treatment of pulmonary arterial hypertension. Curr Clin Pharmacol 2008;3:11-9. Review.

133. Lang RM, Bierig M, Devereux RB, Flachskampf FA, Foster E, Pellikka PA, et al. Recommendations for chamber quantification: a report from the American Society of Echocardiography's Guidelines and Standards Committee and Chamber quantification Writing Group, developed in conjunction with the European Association of Echocardiography, a branch of the European Society of Cardiology. J Am Soc Echocardiogr 2005;18:1440-63.

134. Redington AN, Penny D, Rigby ML, Hayes A. Antegrade diastolic pulmonary artery flow as a marker of right ventricular restriction after complete repair of pulmonary atresia with intact ventricular septum and critical pulmonary valve stenosis. Cardiol Young 1992;2:382-6.

135. Cullen S, Shore D, Redington AN. Characterisation of right ventricular diastolic performance after complete repair of tetrallogy of Fallot. Restrictive physiology predicts slow postoperative recovery. Circulation 1995;91:1782-9.

136. Kisanuki A, Tei C, Otsuji Y, Natsugoe K, Kawazoe Y, Arima S, et al. Doppler echocardiographic documentation of diastolic pulmonary artery forward flow. Am J Cardiol 1987;59:711-3.

137. Wahl A, Praz F, Schwerzmann M et al. Assessment of right ventricular systolic function: Comparison between cardiac magnetic resonance derived ejection fraction and pulsed-wave tissue Doppler imaging of the tricuspid annulus. Int J Cardiol 2010.

138. Uebing A, Gibson DG, Babu-Narayan SV et al. Right ventricular mechanics and QRS durationin in patients with repaired tetralogy of Fallot: implications of infundibular disease. Circulation 2007;116(14):1532-9.

139. Krayenbuehl HP, Hess OM, Ritter M, Monrad ES, Hoppeler H. Left ventricular systolic function in aortic stenosis. Eur Heart J 1988; 9: 19-23.

140. Peterson KL. Tsuji J. Johnson A, DiDonna J, LeWinter M. Diastolic left ventricular pressure-volume and stress-strain relations in patients with valvular aortic stenosis and left ventricular hypertrophy. Circulation 1978; 58: 77-89.

141. Kjaergaard J, Petersen CL, Kjaer A, Schaadt BK, Oh JK, Hassager C. Evaluation of right ventricular volume and function by 2D and 3D echocardiography compared to MRI. Eur J Echocardiogr 2006;7:430-8.

142. Calcutteea A, Chung R, Linqvist P, Hodson M, Henein MY. Differential Right ventricular regional function and the effect of pulmonary hypertension*:* three dimensional echo study. Heart 2011;97:1004-11.

143. Duncan AM, Lim E, Clague J, Gibson DG, Henein MY. Comparison of segmental and global markers of dyssynchrony in predicting clinical response to cardiac resynchronization. Eur Heart J 2006;27:2426-32.

144. Mor-Avi V, Sugeng L, Lindner JR. Imaging the Forgotten Chamber: Is the Devil in the Boundary?. J Am Soc Echocardiogr 2010;23:141-3.

Table 1: Clinical characteristics of patients

Aetiology of PH (n = 35)	Value
Idiopathic pulmonary arterial hypertension (IPAH)	9
Associated pulmonary arterial hypertension (APAH)	14
Pulmonary veno-occlusive disease (PVOD)	2
Chronic thromboembolic pulmonary hypertension (CTEPH)	7
Lung fibrosis	1
Others	2

PH : pulmonary hypertension

Table 2: LV and RV structure and function

	Controls (n = 20)	PHT (n = 35)	p-value
Age, years	62 ± 15	67 ± 12	0.2
Heart rate, bpm	64 ± 9	75 ± 14	0.001
LVEDV, ml	96 ± 14	84 ± 20	0.008
LVESV, ml	37 ± 7	35 ± 10	0.5
LA volume, ml	50 ± 8	51 ± 12	0.16
LVEF %	61 ± 2	57 ± 7	0.02
E/E' (LV)	6 ± 1	7.5 ± 1.5	0.04
RV inlet diameter, cm	3 ± 0.3	4.2 ± 0.5	< 0.001
RVOT end diastolic diameter, cm	2.9 ± 0.3	3.7 ± 0.6	< 0.001
RVOT end systolic diameter, cm	1.8 ± 0.2	3 ± 0.7	< 0.001
Pulmonary ejection acceleration (PAc), ms^{-2}	6.6 ± 1.4	12.2 ± 6.4	0.001
TAPSE, cm	2.7 ± 0.3	1.7 ± 0.6	< 0.001
PASP, mmHg	30 ± 2	67 ± 20	< 0.001
MPI (RV)	0.3 ± 0.1	0.7 ± 0.2	< 0.001
SV, ml	58 ± 9	49 ± 14	0.004

LV = left ventricle; RV = right ventricle; TAPSE = tricuspid annular plane systolic excursion; SV: stroke volume.
PASP, mmHg = pulmonary artery systolic pressure; E/E': Early LV diastolic velocity / early filling velocity from TDI.
LVEF = left ventricular ejection fraction; EDV = end-diastolic volume; ESV = end systolic volume; LA = left atrium
MPI (RV) = RV myocardial performance index.

Table 3: RV intrinsic myocardial function (STE)

	Controls (n = 20)	PHT (n = 35)	p value
Motion			
RV inlet velocity (STE), cm/s	9.9 ± 1.4	7.5 ± 2.4	<0.001
STE parameters			
RV (base) longitudinal strain rate, (1/s)	1.9 ± 0.5	1.3 ± 0.6	<0.001
RV (mid) longitudinal strain rate, (1/s)	1.7 ± 0.4	1 ± 0.4	<0.001
RVOT longitudinal strain rate, (1/s)	1.6 ± 0.9	1.3 ± 0.65	0.1
RV (base) longitudinal displacement (STE), mm	15.8 ± 3.6	8.5 ± 4.7	<0.001
RV (mid) longitudinal displacement (STE), mm	9 ± 3.5	4.9 ± 3.1	<0.001
RVOT longitudinal displacement (STE), mm	1.8 ± 1.1	1.7 ± 1	0.86
Timings			
Time to peak systolic strain rate at base, (ms/bpm)	3.7 ± 0.9	2.7 ± 0.9	<0.001
Time to peak systolic strain rate at mid, (ms/bpm)	3.8 ± 0.9	2.7 ± 0.9	<0.001
Time to peak systolic strain rate at RVOT, (ms/bpm)	3.8 ± 1	3 ± 1.1	0.007
Time to peak displacement at base, (ms/bpm)	6.6 ± 1.1	5 ± 1.6	<0.001
Time to peak displacement at mid, (ms/bpm)	6.6 ± 1.1	5 ± 1.6	<0.001
Time to peak displacement at RVOT, (ms/bpm)	6.6 ± 1.8	3.7 ± 1.3	<0.001

RVOT = right ventricular outflow tract; base = basal segment of right ventricle; mid = mid segment of right ventricle; STE = Speckle tracking echocardiography; RV = right ventricle

Table 4: RV pump time relations

	Controls(n = 20)	PHT (n=35)	P value
RV Filling time (PW), (ms/bpm)	7.4 ± 3.6	5.2 ± 2.5	0.03
Time to peak RV ejection (PW), (ms/bpm)	3.7 ± 0.7	2.8 ± 0.9	0.001
Time to end RV ejection (PW), (ms/bpm)	6.9 ± 1.2	5.6 ± 1.4	0.001
TR duration (CW), (ms/bpm)	5.7 ± 1.3	6.4 ± 1.9	0.3
Time to onset of RV filling (PW), (ms/bpm)	7.2 ± 1.5	7 ± 2	0.8
Time to onset of RV ejection (PW),(ms/bpm)	1.3 ± 0.2	1.2 ± 0.4	0.5
Time to onset of shortening (M-mode), (ms/bpm)	1.7 ± 0.3	1.4 ± 0.4	0.007
Time to peak shortening (M-mode), (ms/bpm)	6.6 ± 0.9	5.6 ± 1.8	0.009

RV = Right ventricle; PW = pulse wave spectral Doppler; TR = tricuspid regurgitation;
CW = continuous wave

Figure 1: Longitudinal strain rate of the base, mid and apical region of the right ventricle.

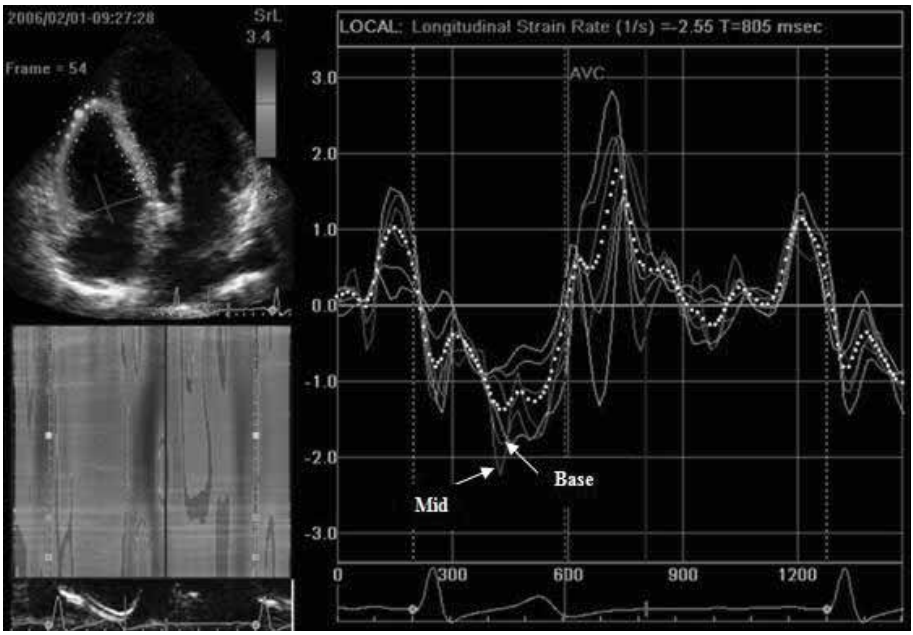

Figure 2: Longitudinal strain rate of the right ventricular outflow tract (RVOT).

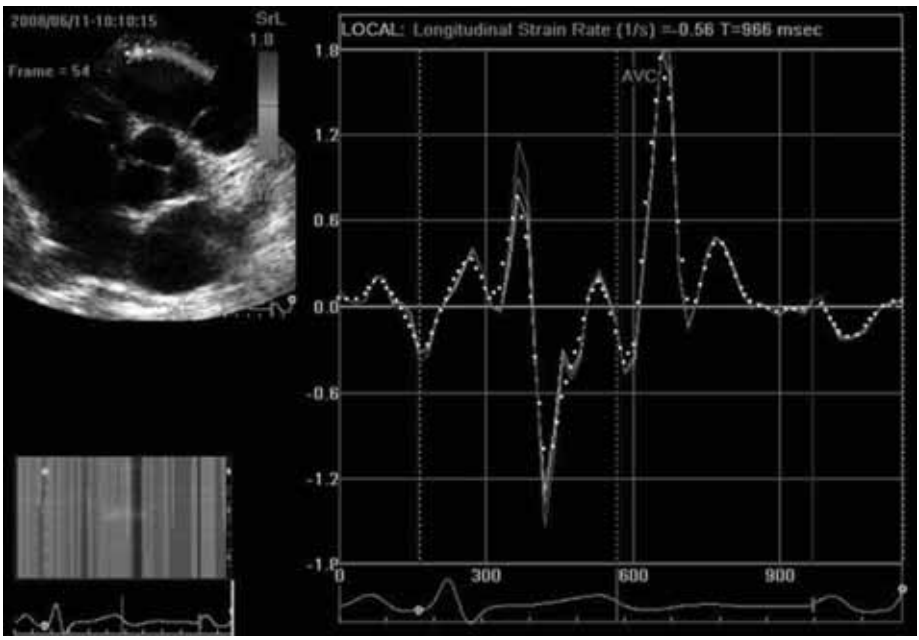

Figure 3: Segmental RVOT correlation with RV ejection in normals

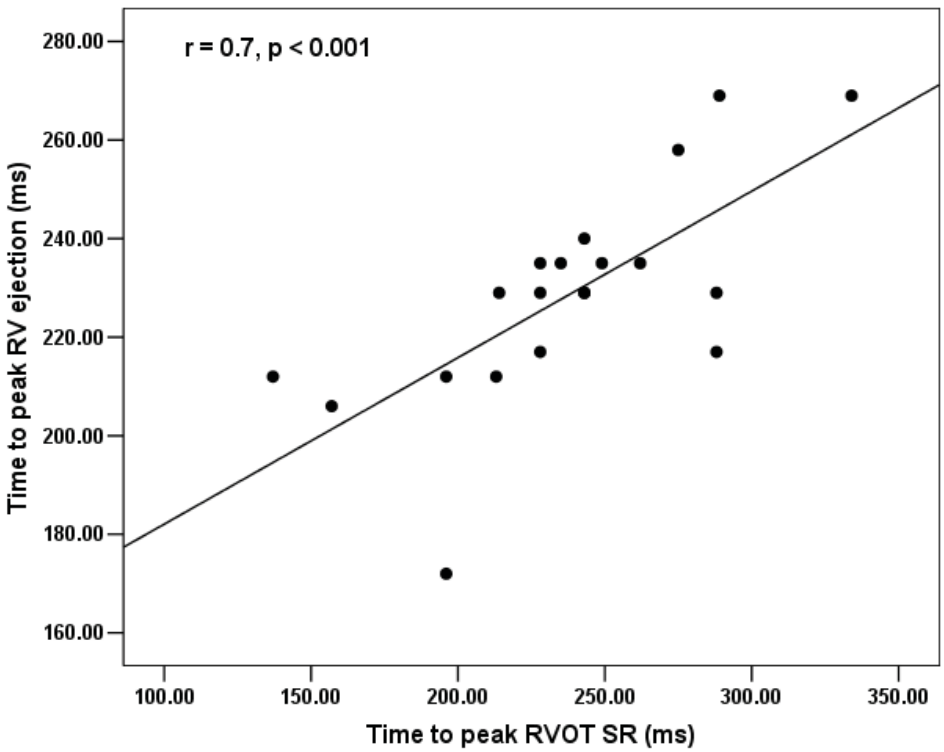

Figure 4: Segmental mid correlation with RV ejection in PH patients.

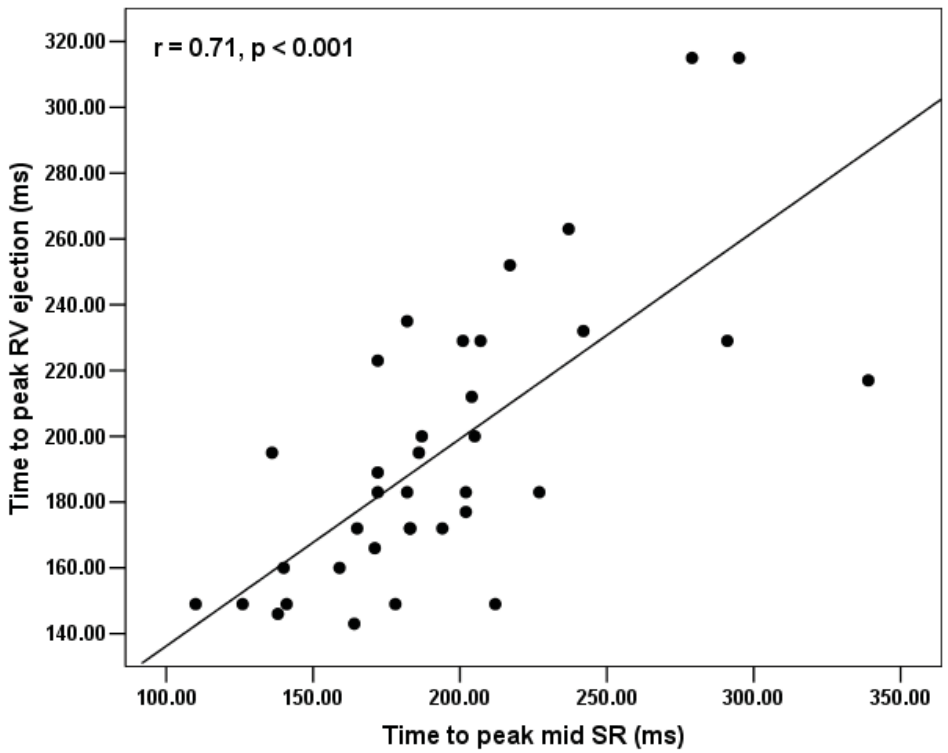

Department of Public Health and Clinical Medicine
Umeå universitet, 901 87 Umeå

ISSN no: 0346-6612
ISBN no: 978-91-7459-561-1
New Series No 1551